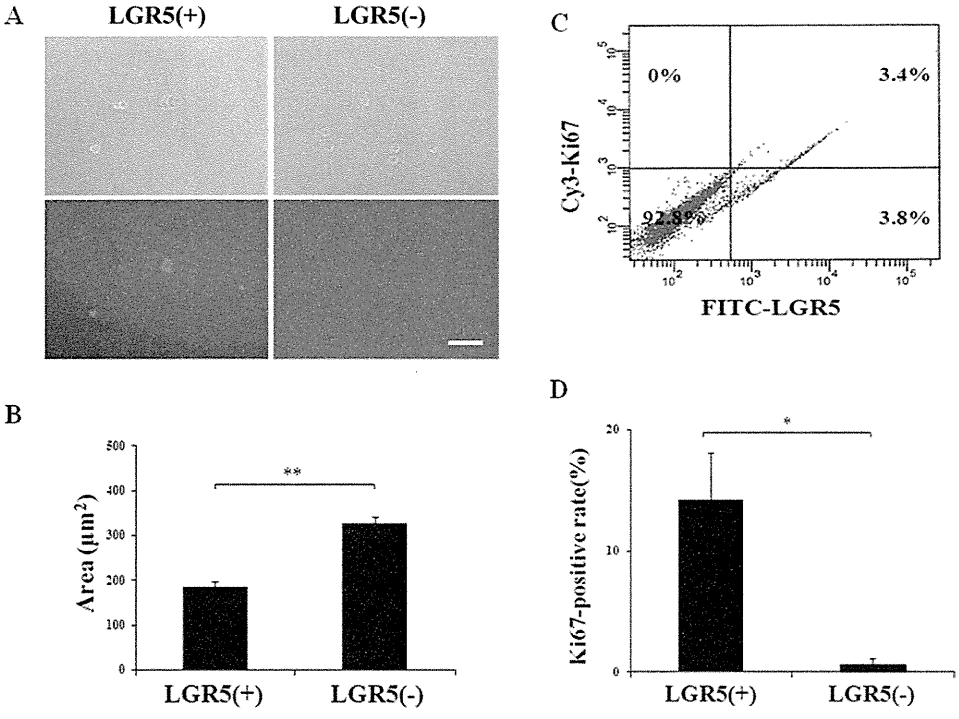

Figure 3. Characterization of leucine-rich repeat G protein-coupled receptor 5 (LGR5$^+$) Monkey corneal endothelial cells. **(A):** Phase contrast image and immunocytochemistry for LGR5 in LGR5$^+$ cells and LGR5(−) cells after cell sorting. Scale bar = 100 μm. **(B):** Average cell size of LGR5$^+$ (184.6 ± 45.8 μm^2) and LGR5$^-$ (326.78 ± 78.8 μm^2). Mean ± SEM. **, $p < .01$. $n = 35$. **(C):** Cell proliferation of LGR5$^+$ by double-immunostaining. LGR5$^+$/Ki67$^+$; 3.4%, LGR5$^+$/Ki67$^-$; 3.8%, LGR5$^-$/Ki67$^+$; 0%, LGR5$^-$/Ki67$^-$; 92.8%. **(D):** Ki67-positive rate of LGR5$^+$ and LGR5$^-$. Mean ± SEM. *, $p < .05$. $n = 4$. Abbreviations: FITC, fluorescein isothiocyanate, LGR5, leucine-rich repeat G protein-coupled receptor 5.

homogeneously hexagonal cells (Fig. 2C). The expression pattern of LGR5 in the monkey CECs closely mimicked that of in the human donor CECs (data not shown). Immunostaining of those cells showed that LGR5 is moderately expressed both in the donor cells and in vitro cells (Fig. 2C), even though the mean *LGR5* mRNA expression in vitro gradually decreased through the cell passages (*$p < .05$) (Fig. 2D). In view of these findings using human and monkey cells, it is likely that LGR5 may play a role in maintaining the cell integrity of CECs.

LGR5$^+$ CECs Were Small and Exhibited Higher Proliferative Potential

To examine the characteristics of the LGR5$^+$ and LGR5$^-$ cell fractions, the subsets were isolated by flow cytometry. To validate the cell sorting procedure, immunofluorescence for LGR5 confirmed its expression at the protein level in the purified fraction (Fig. 3A).

As the highest clonogenicity is reportedly found in the smallest keratinocytes [28], the cell size in each isolated fraction was measured by use of Scion Image software. Viewed under an inverted microscope, the LGR5$^+$ cells were found to be clearly smaller than the LGR5$^-$ cells (Fig. 3B), and the average size of the LGR5$^+$ cells was significantly smaller than that of the LGR5$^-$ cells (184.6 ± 45.8 μm^2 vs. 326.78 ± 78.8 μm^2, respectively, $n = 35$, **$p < .01$).

Next, to assess the cell-cycling status of each isolated cell fraction, FACS was used for double-staining with LGR5 and Ki67. FACS analysis showed that the LGR5^{high}/Ki67^{high} cell fraction was 3.4%, whereas the LGR5^{high}/Ki67^{low} cell fraction was 3.8% (Fig. 3C). Most interestingly, all LGR5^{low} cell fractions showed the Ki67 low level (92.8%). To further examine the proliferative capacity of each isolated cell fraction in detail, isolated cell fractions were cultivated on cell chamber slides. Five days later in culture, the percentage of Ki67-labeled cells in the LGR5$^+$ and LGR5$^-$ cells was 14.2 ± 3.87% and 0.58 ± 0.5%, respectively, rendering the difference in the Ki67-labeling index statistically significant (*$p < .05$) (Fig. 3D), suggesting that without the LGR5 expression, CECs do not have proliferative ability.

Active HH Signaling Induced LGR5 Expression

HH signaling reportedly plays a key role in various kinds of biological processes, such as cell differentiation, proliferation, and growth [16, 29, 30]. To define the properties of LGR5 in CECs at the molecular level, we first examined the expression of HH signaling-related molecules in human donor CECs. Of interest, the levels of *SHH*, *Gli1*, and *Gli2* mRNA were found to be elevated in CECs located in the peripheral-region as compared to those in the central region (Fig. 4A). On the other hand, the expression level of smoothened (*Smo*) and protein patched homolog one (*Ptch1*) receptor molecules in the HH pathway was similar (Fig. 4A). Thus, HH signaling was clearly activated in the peripheral-region CECs, suggesting that a regional variation of HH signaling activity does exist.

To determine whether the expression of LGR5 in the CECs was regulated by the HH signaling pathway, the peripheral donor CECs (outside the 8-mm central cornea area) were incubated in culture medium (Dulbecco's modified Eagle's medium + 5% FBS) and stimulated using recombinant SHH (an HH ligand, 100 ng/ml), purmorphamine (an HH agonist, 2 μM) [31], and cyclopamine (an HH antagonist, 2 μM) [32] for 24 hours at 37°C in 5% CO_2. As expected, expression of *LGR5* in the peripheral-region CECs, yet not in the central-region CECs, was found to be upregulated by SHH and

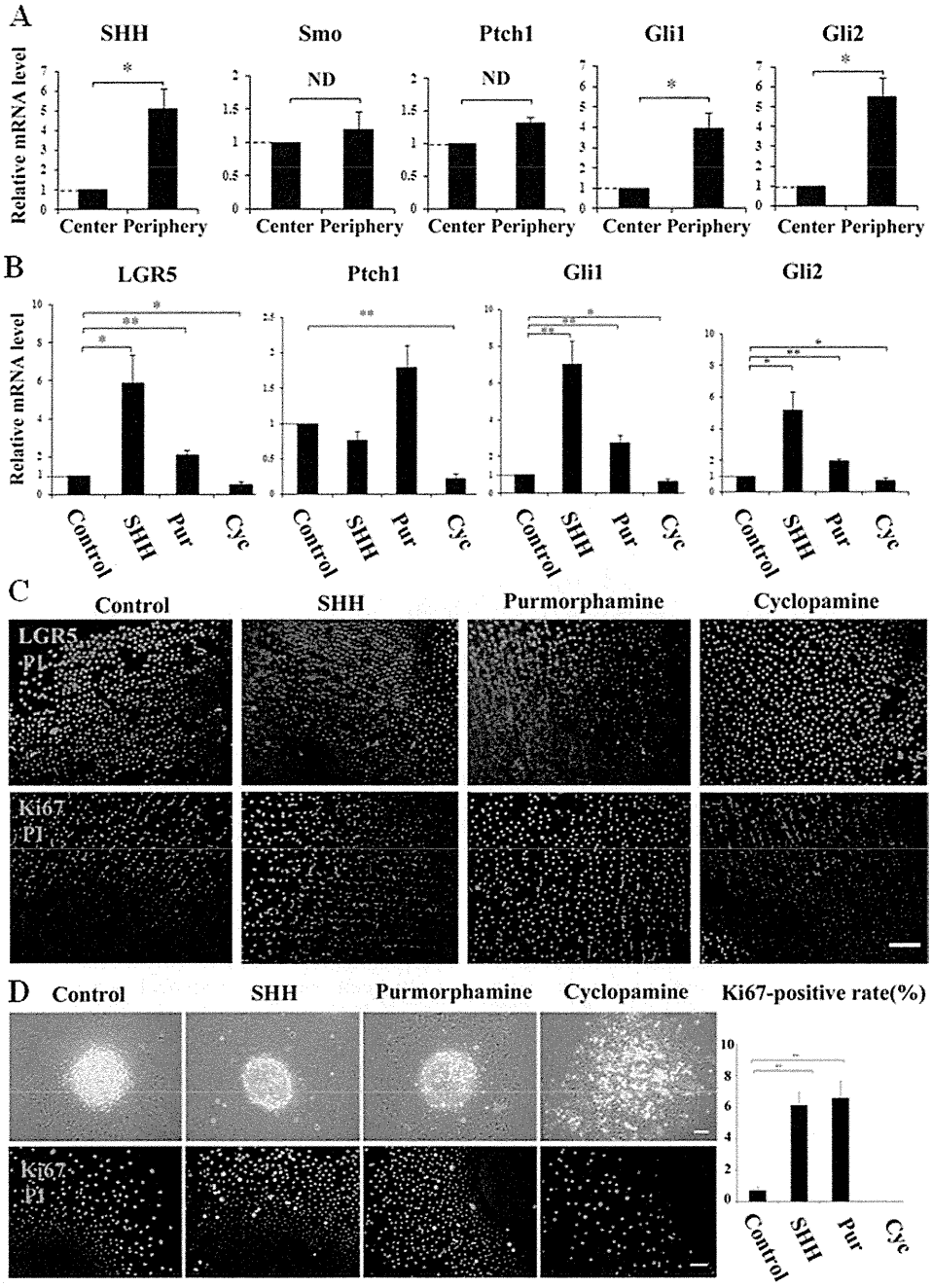

Figure 4. Hedgehog (HH) signaling pathway in corneal endothelial cells (CECs). **(A):** Real-time polymerase chain reaction (PCR) for HH signal-associated genes (*SHH*, *Smo*, *Ptch1*, *Gli1*, and *Gli2*) in central and peripheral human donor CECs. Mean ± SEM. *, $p < .05$. $n = 4$. **(B):** Real-time PCR of leucine-rich repeat G protein-coupled receptor 5 (*LGR5*), *Ptch1*, *Gli1*, and *Gli2* in human donor CECs treated with SHH, purmorphamine (Pur), and cyclopamine (Cyc), respectively. Mean ± SEM. *, $p < .05$; **, $p < .01$. $n = 4$. **(C):** Immunostaining of LGR5 and Ki67 in human donor CECs treated with SHH, Pur, and Cyc, respectively. Control: 0.1% dimethyl sulfoxide (DMSO). Scale bar = 100 μm. **(D):** Immunostaining of Ki67 in cultivated human CECs treated with SHH, Pur, and Cyc, respectively. Control: 0.01% DMSO. Scale bar = 100 μm. Ki67-positive rate of human CECs treated with SHH, Pur, and Cyc, respectively. Mean ± SEM. **, $p < .01$. $n = 5$. Abbreviations: LGR5, leucine-rich repeat G protein-coupled receptor 5; mRNA, messenger RNA; ND, No significant difference; PI, propidium iodide; SHH, sonic Hedgehog.

purmorphamine stimulation, whereas *LGR5* expression was reduced by cyclopamine stimulation at both the mRNA and protein levels (Fig. 4B, 4C). The expression patterns of *Gli1* and *Gli2* were similar to that of *LGR5*, but HH activation did not dramatically have an influence on *Ptch1*, the HH receptor (Fig. 4B).

Next, immunohistochemistry for Ki67 was performed to elucidate whether or not the HH pathway induced donor CEC proliferation. As human CECs are mitotically inactive and show weak-to-no proliferative capacity *in vivo* [3], an elevated expression of Ki67 was not observed in all experimental groups, suggesting that stimulation of the HH pathway alone is not sufficient to induce donor CEC proliferation (Fig. 4C). However, CECs reportedly retain the capacity to proliferate in vitro [4], so we investigated whether the HH pathway induced CEC proliferation in vitro. The expression of Ki67 was found

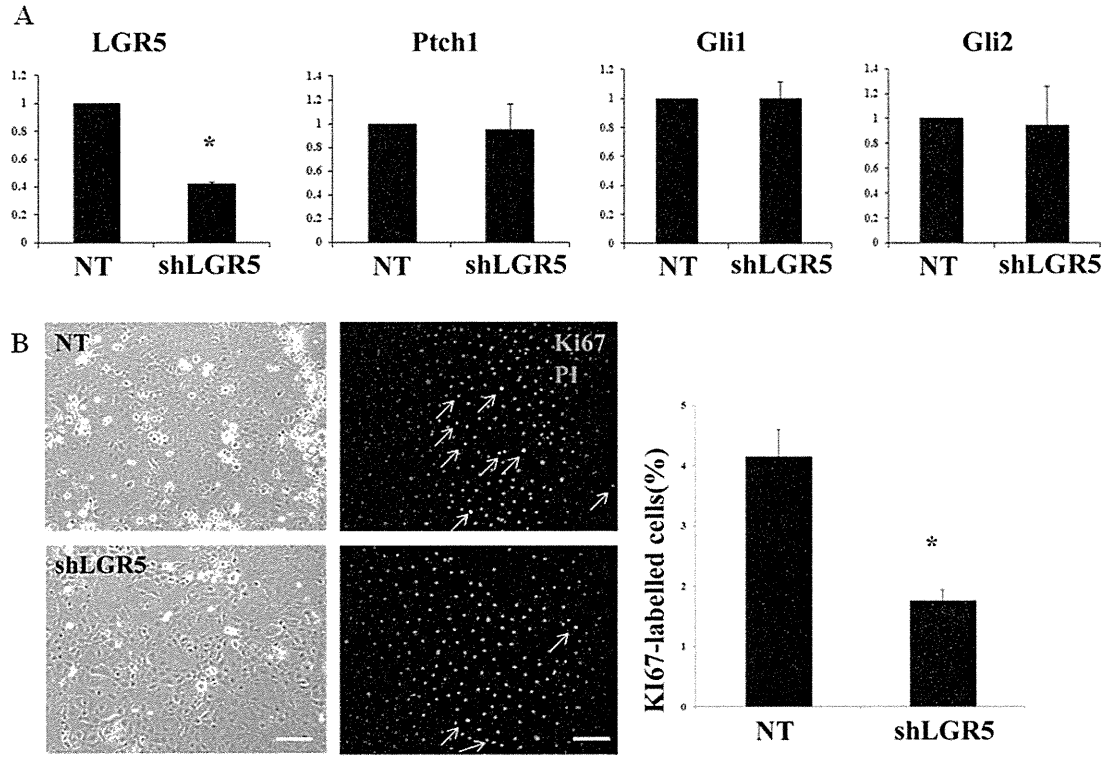

Figure 5. Effect of short hairpin *LGR5* (shLGR5) in human corneal endothelial cells (CECs). **(A):** Real-time polymerase chain reaction for leucine-rich repeat G protein-coupled receptor 5 (*LGR5*), *Ptch1*, *Gli1*, and *Gli2* in nontarget (NT)- and shLGR5-transfected cells. Mean ± SEM. *, $p < .05$. $n = 3$. **(B):** Phase contrast microscopy image and immunostaining of Ki67 in NT- and shLGR5-transfected human CECs. Arrows point to $Ki67^+$ cells. Scale bar = 100 μm. Mean ± SEM. *, $p < .05$. $n = 5$. Abbreviations: LGR5, leucine-rich repeat G protein-coupled receptor 5; NT, nontarget; PI, propidium iodide; shLGR5, short hairpin LGR5.

to be upregulated in response to SHH- and purmorphamine-stimulation, however, it was not upregulated in response to cyclopamine (Fig. 4D). These findings indicate that in the in vitro situation, the HH pathway is able to induce CEC proliferation. We posit that CECs treated with cyclopamine were unable to maintain their normal hexagonal morphology (Fig. 4D). Furthermore, Real-time PCR showed that the expression of *LGR5* in the cultured CECs with SHH stimulation was elevated as compared to those without SHH stimulation. Immunohistochemistry showed that after SHH stimulation, the expression of LGR5 in the cultured CECs was elevated in some of the cells, yet not in all of the cells (supplemental online Fig. 1). In view of these findings, we discovered for the first time that LGR5 is the target molecule of HH signaling in CECs and that CEC maintenance is partially regulated by the HH pathway.

Downregulation of LGR5 Decreased the Proliferation of CECs

The direct effect of LGR5 on the CECs was elucidated by the knockdown of *LGR5* by shRNA. For this experiment, primate cultivated CECs were used, due to the fact that cultured human CECs rarely express LGR5 (Fig. 2A, 2B). Nine sets of shRNA were designed, and the efficacy of their knockdown potential was then examined. Of those, shRNA-589 was found to be the most effective for knocking down the *LGR5* mRNA expression (approximately 60% knockdown) (Fig. 5A). Real-time PCR for *Ptch1, Gli1, and Gli2* showed that no significant differences were found between the short hairpin *LGR5* (shLGR5) group and the control (Fig. 5A). To demonstrate the effect of knocking down the *LGR5* gene on CEC proliferation, immunocytochemistry for Ki67 was performed. Compared with the control, cell morphology of the shLGR5-treated cells was not dramatically changed, however, the number of $Ki67^+$ cells in the shLGR5-treated cells was greatly reduced (Fig. 5B). These findings indicated that downregulation of *LGR5* did not have an effect on the HH pathway, but did decrease CEC proliferation in vitro.

Persistent *LGR5* Expression Inhibited MT Through the Wnt Pathway

To investigate the direct effects of persistent *LGR5* expression on CECs, we attempted to overexpress LGR5 using lentivirus containing CMV-*LGR5*- mRFP. In this experiment, human cultivated CECs (fourth passage, 62-year-old donor) were used, as they rarely express LGR5 (Fig. 2A). Real-time PCR showed that the expression of *LGR5* in *LGR5*-transfected cells (6 days after transfection) was about 60 times higher than that in NT vector-transfected cells ($p < .01$) (Fig. 6B). Immunofluorescence was used to confirm that the expression of *LGR5* in the LGR5-transfected cells was elevated in comparison with that in the NT cells (Fig. 6A). Of great interest, the relative mRNA levels of the HH signaling molecules in *LGR5*-transfected cells were downregulated as compared to those in the NT cells (Fig. 6B), indicating that LGR5 operates as a negative feedback regulator of the HH pathway.

Human CECs are reportedly vulnerable to morphological fibroblastic change under normal culture conditions [5]. To better demonstrate the effect of persistent *LGR5* expression, we used fourth-passaged cultivated CECs. After lentivirus transfection, some of the NT cells still exhibited an enlarged and elongated shape (fibroblastic change) (Fig. 6A). Of great

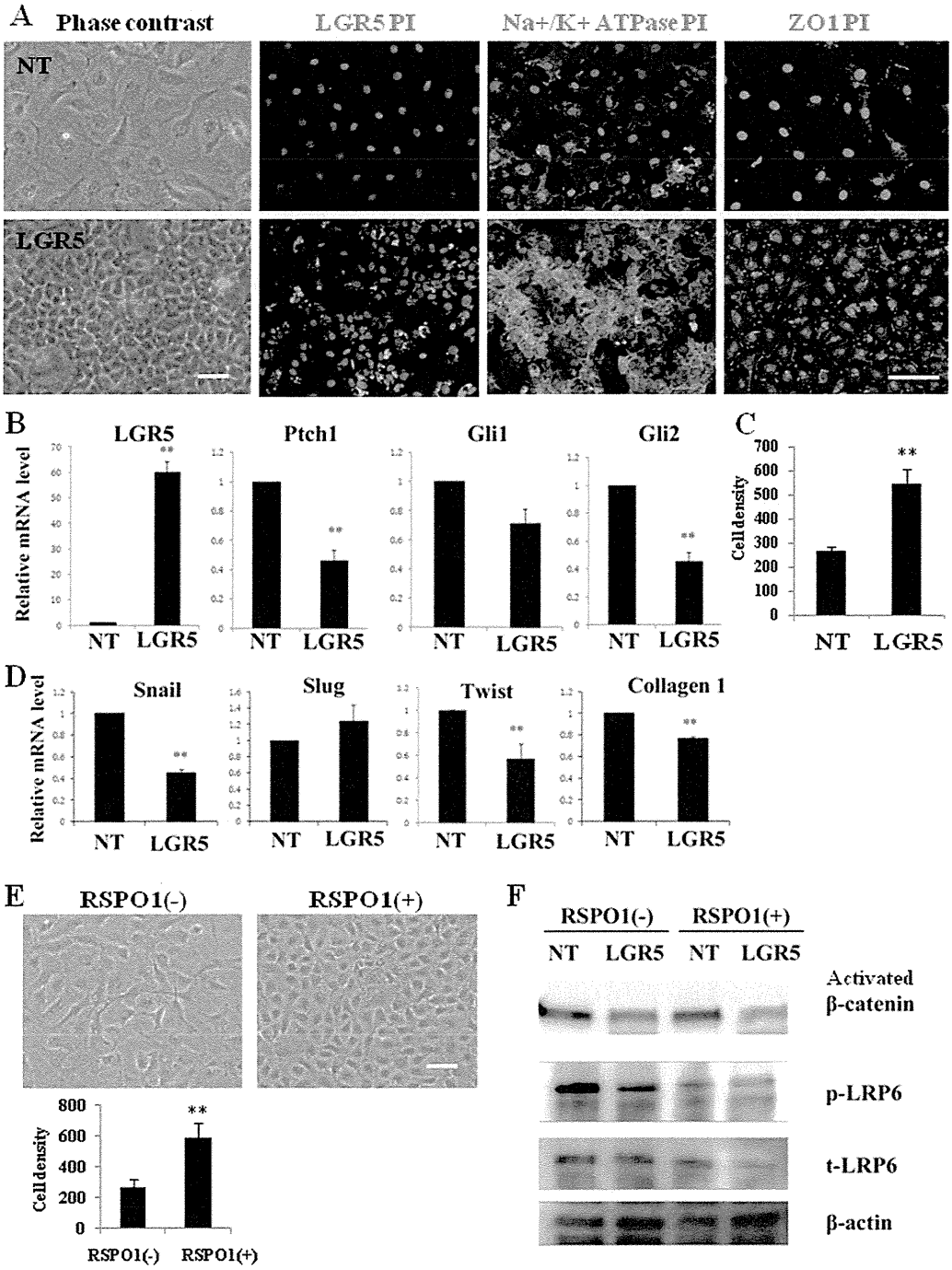

Figure 6. Function of leucine-rich repeat G protein-coupled receptor 5 (LGR5) and R-spondin-1 (RSPO1) in corneal endothelial cells (CECs). **(A):** Phase contrast microscopy image and immunostaining of LGR5, Na+/K+ ATPase, and ZO1 in nontarget (NT)- and *LGR5*-transfected human CECs. Scale bar = 100 μm. **(B):** Relative expression of *LGR5, Ptch1, Gli1, and Gli2* messenger RNA in NT- and *LGR5*-transfected cells. Mean ± SEM. **, $p < .01$. $n = 3$. **(C):** Cell density of NT- and *LGR5*-transfected cells. Mean ± SEM. **, $p < .01$. $n = 5$. **(D):** Real-time polymerase chain reaction for EMT-associated genes (*Snail, Slug, Twist, and collagen1*) in NT- and *LGR5*-transfected cells. Mean ± SEM. **, $p < .01$. $n = 3$. **(E):** Phase contrast image of human cultivated CECs with or without RSPO1 (50 ng/ml). Scale bar = 100 μm. Cell density of CECs with or without RSPO1. Mean ± SEM. **, $p < .01$. $n = 5$. **(F):** Western blotting of activated β-catenin, pLRP6, tLRP6, and β-actin in NT- and LGR5-transfected cells with or without RSPO1 (50 ng/ml). Abbreviations: LGR5, leucine-rich repeat G protein-coupled receptor 5; mRNA, messenger RNA; NT, nontarget; PI, propidium iodide; RSPO, R-spondin-1.

interest, the *LGR5*-transfected cells gradually changed their morphology and were shown to be compact, smaller-size, homogeneously hexagonal cells, resuming the normal physiological morphology (Fig. 6A). Cell density of the *LGR5*-transfected cells was found to be greatly elevated compared with that of the NT cells (Fig. 6C). To examine the function of cultivated CECs transfected with the NT and *LGR5* vector, immunohistochemistry was performed for Na^+/K^+ ATPase and ZO1. The expression of these two functional proteins was found to be much greater in the *LGR5*-transfected cells than in the NT cells, even though these expression patterns were not typical in comparison with those in in vivo CECs (Fig.

6A). In view of these findings, it is likely that LGR5 may be the key molecule for maintaining normal CEC phenotypes.

Transformation of endothelial cells to fibroblastic cells is known as endothelial–mesenchymal transformation (MT) [33]. The interesting findings observed in the *LGR5*-transfected cells led us to further study whether or not the persistent expression of *LGR5* was able to block the MT process. The expression level of epithelial-MT (EMT)-related molecules (*Snail, Slug, Twist, and Collagen1*) [34] was examined using real-time PCR. Of great importance, the relative mRNA level of all EMT markers except Slug were lower in the *LGR5*-transfected cells than in the NT cells (Fig. 6D), suggesting that persistent *LGR5* expression blocked the MT process. We further examined which pathway regulates the endothelial-MT observed in CECs. Recent studies suggest that the Wnt/β-catenin signaling pathway plays an important role in EMT [34]. Therefore, the expression level of Wnt/β-catenin-related molecules was examined using western blot analysis. Worthy of note, the protein level of cytosolic (non membrane bound) β-catenin and phosphorylated low-density-lipoprotein receptor-related protein 6 (p-LRP6) was greatly decreased in the LGR5-transfected cells (Fig. 6F). We found that the expression of β-catenin shifted from the cell membrane to the cytoplasm and nucleus, which is well observed in the typical EMT process, in most of nontarget transfected CECs. In contrast, we could observe the expression of β-catenin in cell membrane of LGR5-transfected CECs (supplemental online Fig. 2). These findings indicated that persistent LGR5 expression inhibited the corneal endothelial-MT through the Wnt/β-catenin pathway.

RSPO1-Accelerated CEC Proliferation and Inhibited MT Through the Wnt Pathway

Previously, LGR5 was thought to be an orphan receptor of the G protein-coupled receptor superfamily, and its ligand was unknown. However, several recent reports demonstrated that RSPOs function as ligands of LGR5 to regulate Wnt/β-catenin signaling [35–37]. Interestingly, we discovered that *RSPO1*, *2*, *3*, and *4* mRNA were expressed in the corneal epithelium, stroma, and endothelium, and that *RSPO1*, *2*, and *3* mRNA were only expressed in the peripheral-region CECs (supplemental online Fig. 3A). To determine the function of RSPOs on CEC differentiation, we cultured the primary human CECs with or without human recombinant RSPOs. Worthy of note, 7 days after culture, only cultivated human CECs treated with RSPO1 [50 ng/ml] showed the compact, smaller-size, homogeneously hexagonal cells, whereas other RSPOs did not have an obvious effect on CEC differentiation in vitro (supplemental online Fig. 3B). To determine the function of RSPOs on donor CEC proliferation, we performed immunohistochemistry for Ki67. Most surprisingly and very interestingly, human donor CECs incubated with RSPO1 (50 ng/ml) for 48 hours at 37°C showed a dramatically increased level of $Ki67^+$ cell ratios as compared to other RSPOs (supplemental online Fig. 3C). In view of these findings, we think that among the RSPOs family, RSPO1 in particular may play an important role in the maintenance of CECs.

Finally, to further determine the effect of RSPO1 on CECs, we maintained the secondary culture of human CECs with or without RSPO1. Through culturing the CECs in both conditions, we clearly observed that the cultured cells with RSPO1 maintained their hexagonal morphology, whereas some of the cultured cells without RSPO1 still showed fibroblastic phenotypes (Fig. 6E). Moreover, the cell density of RSPO1-treated cells was elevated in comparison with that of the nontreated cells (Fig. 6E). To demonstrate which pathway regulates this type of corneal endothelial MT, we examined the expression level of Wnt/β-catenin-related molecules using western blot analysis. We performed the experiments twice, and the results were nearly identical; the protein level of cytosolic β-catenin and p-LRP6 in the LGR5-transfected cells treated with RSPO1 was decreased in comparison with that in the NT cells (Fig. 6F). Moreover, the protein levels of the RSPO1-treated NT and LGR5-transfected cells were more decreased as compared to the cells not treated with RSPO1 (Fig. 6F). These results suggested that the stimulation of cells overexpressing LGR5 with RSPO1 accelerates pLRP degradation and β-catenin turnover.

Discussion

Cornea tissue is extremely important, as most mammals acquire the majority of their external information through it. Recently, particular attention has been focused on CECs due to the fact that the corneal transplantation procedure is currently undergoing a paradigm shift from keratoplasty to endothelial keratoplasty. Therefore, both scientifically and clinically, to establish the next generation of novel therapy for treating cornea-related blindness worldwide, it is extremely important to understand the molecular mechanism of corneal endothelial stem/progenitor cells. However, very little is presently known about those molecular mechanisms.

It has been reported that the characteristics and proliferative potential of CECs are different between those located at the central region of the cornea and those located at the peripheral region of the cornea [38, 39], and a study has shown that the cornea has a higher density of endothelial cells in the peripheral region than in the central region [40]. Moreover, CECs from the peripheral region reportedly retain higher replication ability than those from the central region [12], and peripheral-region CECs contain more precursors and have a stronger self-renewal capacity than CECs in the central region [41]. He et al. recently identified a novel anatomic organization in the peripheral region of human corneal endothelium, suggesting a continuous slow centripetal migration of CECs from specific niches [15]. Thus, it is most likely that human corneal endothelial stem/progenitor cells are mainly distributed in the peripheral region. In fact, no stem/progenitor cell marker for CECs has thus-far been elucidated, and the results of this study demonstrate for the first time that CECs exhibit regional diversity with respect to LGR5 expression. In view of these findings and the unique expression pattern of LGR5 in CECs, LGR5 might represent a first marker for corneal endothelial stem-cell-containing populations.

It has been reported that cell size may distinguish keratinocyte stem cells from transient amplifying cells or differentiated cells [28]. In the epidermis, the response to phorbol esters of the smallest keratinocytes is different from that of other cells. Those keratinocytes also exhibited the highest clonogenicity. Even though CECs are different from ectoderm-derived keratinocytes, the average diameter of the $LGR5^+$ cells in this study was in fact smaller than that of the $LGR5^-$ cells. Based on these findings, and on the findings of the above-cited previous report regarding the size of peripheral CECs, it is possible that cell size might be a potential indicator of corneal endothelial stem/progenitor cells.

We found that LGR5 is a key molecule for maintaining the integrity of CECs and regulating normal cell phenotypes in vitro. We also found that isolated cells fractionated based on the intensity of their LGR5 expression could produce different cell populations with different properties. Only cells in

the LGR5$^+$ population exhibited exceptionally high proliferative potential, features associated with stem/progenitor cell populations. Based on these findings, the unique expression pattern and necessity in the in vitro condition, there is possibly a link between LGR5 and the function of corneal endothelial stem/progenitor cells.

Previous studies have indicated that high concentration of SHH caused a marked increase in retinal progenitor cell proliferation and a general increase in the accumulation of differentiated cells [29]. The findings of this present manuscript show that in the in vitro situation, the HH pathway is able to induce CEC proliferation, consistent with the findings of previous reports. HH is a family of secreted molecules that serve as morphogens during multiple aspects of development in a wide range of tissue types. HH is involved in the left-right asymmetry decision and anterior–posterior axis decision in limb pattern determination by regulating cell proliferation and survival. In CECs, there is regional variation of HH signal activity, and based on our findings, HH signaling might possibly control corneal endothelial morphogenesis.

RSPOs are a family of four cysteine-rich secreted proteins that were isolated as strong potentiators of Wnt/β-catenin signaling. A vast amount of information regarding the cell biological functions of RSPOs has emerged over the last several years, especially with respect to their role as ligands of the orphan receptors LGR 4/5/6. These updated and important findings led us to further study whether RSPOs may have an effect on the function of human CECs. As human CECs are mitotically inactive and are essentially nonregenerative in vivo, corneal endothelial loss due to disease or trauma is followed by a compensatory enlargement of the remaining endothelial cells. To the best of our knowledge, there are no reports regarding a useful inductive reagent or molecule to increase the level of human CEC proliferation and CEC density, although we previously developed the CECs culture protocol using Y-27632 [21, 22]. We examined the expression of RSPO1 in CECs and found that its protein level is quite low (data no shown), suggesting that external RSPO1, rather than internal RSPO1, plays a critical role in maintaining the CEC function. Moreover, although there was no expression of LGR5 in the cultured CECs, RSPO1 did have some effect on the condition of CECs in vitro. We do not precisely know the reason why, but from our results, we presume that the effect of RSPO1 on CECs might be of both an LGR5-dependent and -independent manner. The findings of this study show for the first time that CECs incubated with RSPO1 exhibited a dramatically increased level of cell proliferation and cell density, suggesting that it might represent a first candidate molecule for reconstructing the damaged cornea through topical application or for use as a culture reagent.

Several studies suggest that the Wnt/β-catenin pathway plays an important role in EMT and that activation of Wnt/β-catenin-dependent signaling modulates the expression of EMT-related genes [34]. However, previous reports have indicated that RSPOs potentiate Wnt/β-catenin signaling by actually functioning as a ligand of LGR5 [35–37]. The exact mechanism involved in this activation is still unclear and there are several conflicting findings as to whether LGR5 is a positive or negative regulator of the Wnt pathway [42–44]. One possible explanation is that the molecular mechanism depends on the tissues, organs, and the species of animal. The cornea is a unique avascular tissue, and its health is maintained by tears and aqueous humor. In contrast, the health of most other organs is maintained by vascular support, suggesting that the characteristics and mechanism of corneal cells are fundamentally different from the epithelial cells of other tissues. Thus, based on the findings of this study, RSPO1 dramatically accelerates CEC proliferation and inhibits corneal endothelial MT through the Wnt pathway.

Conclusion

In conclusion, the findings of this study are the first to demonstrate the function of LGR5 in human CECs (supplemental online Fig. 4). LGR5 has proven to be a powerful tool in identifying a multitude of stem/progenitor cell populations. Through the regulation of LGR5 through the HH and Wnt pathways, CEC integrity was well structured and maintained. In addition, the LGR5 ligand RSPO1 may exploit the novel substantial protocol to provide the efficient expansion of CECs, suggesting that RSPO1-based three dimensional culture and medical treatments hold promise for regenerative therapy, not only for the treatment of corneal dysfunctions, but also for a variety of severe general diseases.

Acknowledgments

The authors wish to thank Yuiko Hata, Rie Yasuda, Kenta Yamazaki, Yuji Sakamoto, and Shoki Okura for assisting with the experimental procedures, and John Bush for reviewing the manuscript. Drs. Noriko Koizumi and Shigeru Kinoshita had applied for the patent regarding the use of ROCK inhibitor on corneal endothelial research (WO/2009/028631). This study was supported in part by Grants-in-Aid for scientific research from the Highway Program for realization of regenerative medicine, the JST-ETH Strategic Japanese-Swiss Cooperative Program and OptiStem.

Disclosure of Potential Conflicts of Interest

The authors indicate no potential conflicts of interest.

References

1 Whitcher JP, Srinivasan M, Upadhyay MP. Corneal blindness: a global perspective. Bull World Health Organ 2001;79:214–221.
2 Tan DT, Dart JK, Holland EJ et al. Corneal transplantation. Lancet 2012;379:1749–1761.
3 Joyce NC. Proliferative capacity of the corneal endothelium. Prog Retin Eye Res 2003;22:359–389.
4 Engelmann K, Bohnke M, Friedl P. Isolation and long-term cultivation of human corneal endothelial cells. Invest Ophthalmol Vis Sci 1988; 29:1656–1662.
5 Peh GS, Beuerman RW, Colman A et al. Human corneal endothelial cell expansion for corneal endothelium transplantation: an overview. Transplantation 2011;91:811–819.
6 Blanpain C, Horsley V, Fuchs E. Epithelial stem cells: turning over new leaves. Cell 2007;128:445–458.
7 De Luca M, Pellegrini G, Green H. Regeneration of squamous epithelia from stem cells of cultured grafts. Regen Med 2006;1:45–57.
8 Lavker RM, Sun TT. Epithelial stem cells: the eye provides a vision. Eye (Lond) 2003;17:937–942.
9 Cotsarelis G, Cheng SZ, Dong G et al. Existence of slow-cycling limbal epithelial basal cells that can be preferentially stimulated to proliferate: implications on epithelial stem cells. Cell 1989;57: 201–209.

10 Pellegrini G, Golisano O, Paterna P et al. Location and clonal analysis of stem cells and their differentiated progeny in the human ocular surface. J Cell Biol 1999;145:769–782.
11 Schermer A, Galvin S, Sun TT. Differentiation-related expression of a major 64K corneal keratin in vivo and in culture suggests limbal location of corneal epithelial stem cells. J Cell Biol 1986;103: 49–62.
12 Mimura T, Joyce NC. Replication competence and senescence in central and peripheral human corneal endothelium. Invest Ophthalmol Vis Sci 2006;47:1387–1396.
13 Whikehart DR, Parikh CH, Vaughn AV et al. Evidence suggesting the existence of stem cells for the human corneal endothelium. Mol Vis 2005;11:816–824.
14 McGowan SL, Edelhauser HF, Pfister RR et al. Stem cell markers in the human posterior limbus and corneal endothelium of unwounded and wounded corneas. Mol Vis 2007;13:1984–2000.
15 He Z, Campolmi N, Gain P et al. Revisited microanatomy of the corneal endothelial periphery: new evidence for continuous centripetal migration of endothelial cells in humans. Stem Cells 2012;30: 2523–2534.
16 Barker N, van Es JH, Kuipers J et al. Identification of stem cells in small intestine and colon by marker gene Lgr5. Nature 2007;449: 1003–1007.
17 Jaks V, Barker N, Kasper M et al. Lgr5 marks cycling, yet long-lived, hair follicle stem cells. Nat Genet 2008;40:1291–1299.
18 Barker N, Huch M, Kujala P et al. Lgr5(+ve) stem cells drive self-renewal in the stomach and build long-lived gastric units in vitro. Cell Stem Cell 2010;6:25–36.
19 Tanese K, Fukuma M, Yamada T et al. G-protein-coupled receptor GPR49 is up-regulated in basal cell carcinoma and promotes cell proliferation and tumor formation. Am J Pathol 2008;173:835–843.
20 Koizumi N, Okumura N, Kinoshita S. Development of new therapeutic modalities for corneal endothelial disease focused on the proliferation of corneal endothelial cells using animal models. Exp Eye Res 2012;95:60–67.
21 Koizumi N, Sakamoto Y, Okumura N et al. Cultivated corneal endothelial cell sheet transplantation in a primate model. Invest Ophthalmol Vis Sci 2007;48:4519–4526.
22 Okumura N, Koizumi N, Ueno M et al. ROCK inhibitor converts corneal endothelial cells into a phenotype capable of regenerating in vivo endothelial tissue. Am J Pathol 2012;181:268–277.
23 Nakamura T, Endo K, Kinoshita S. Identification of human oral keratinocyte stem/progenitor cells by neurotrophin receptor p75 and the role of neurotrophin/p75 signaling. Stem Cells 2007;25:628–638.
24 Nakamura T, Ohtsuka T, Sekiyama E et al. Hes1 regulates corneal development and the function of corneal epithelial stem/progenitor cells. Stem Cells 2008;26:1265–1274.
25 Nakatsukasa M, Kawasaki S, Yamasaki K et al. Tumor-associated calcium signal transducer 2 is required for the proper subcellular localization of claudin 1 and 7: implications in the pathogenesis of gelatinous drop-like corneal dystrophy. Am J Pathol 2010;177: 1344–1355.
26 Aghib DF, McCrea PD. The E-cadherin complex contains the src substrate p120. Exp Cell Res 1995;218:359–369.
27 Van Horn DL, Hyndiuk RA. Endothelial wound repair in primate cornea. Exp Eye Res 1975;21:113–124.
28 Barrandon Y, Green H. Cell size as a determinant of the clone-forming ability of human keratinocytes. Proc Natl Acad Sci U S A 1985;82:5390–5394.
29 Stanton BZ, Peng LF. Small-molecule modulators of the Sonic Hedgehog signaling pathway. Mol Biosyst 2010;6:44–54.
30 Tsuru T, Araie M, Matsubara M et al. Endothelial wound-healing of monkey cornea: fluorophotometric and specular microscopic studies. Jpn J Ophthalmol 1984;28:105–125.
31 Sinha S, Chen JK. Purmorphamine activates the Hedgehog pathway by targeting Smoothened. Nat Chem Biol 2006;2:29–30.
32 Chen JK, Taipale J, Cooper MK et al. Inhibition of Hedgehog signaling by direct binding of cyclopamine to Smoothened. Genes Dev 2002;16:2743–2748.
33 Lee HT, Lee JG, Na M et al. FGF-2 induced by interleukin-1 beta through the action of phosphatidylinositol 3-kinase mediates endothelial mesenchymal transformation in corneal endothelial cells. J Biol Chem 2004;279:32325–32332.
34 Lee JM, Dedhar S, Kalluri R et al. The epithelial-mesenchymal transition: new insights in signaling, development, and disease. J Cell Biol 2006;172:973–981.
35 Carmon KS, Gong X, Lin Q et al. R-spondins function as ligands of the orphan receptors LGR4 and LGR5 to regulate Wnt/beta-catenin signaling. Proc Natl Acad Sci U S A 2011;108:11452–11457.
36 de Lau W, Barker N, Low TY et al. Lgr5 homologues associate with Wnt receptors and mediate R-spondin signalling. Nature 2011;476: 293–297.
37 Glinka A, Dolde C, Kirsch N et al. LGR4 and LGR5 are R-spondin receptors mediating Wnt/beta-catenin and Wnt/PCP signalling. EMBO Rep 2011;12:1055–1061.
38 Bednarz J, Rodokanaki-von Schrenck A, Engelmann K. Different characteristics of endothelial cells from central and peripheral human cornea in primary culture and after subculture. In Vitro Cell Dev Biol Anim 1998;34:149–153.
39 Patel SP, Bourne WM. Corneal endothelial cell proliferation: a function of cell density. Invest Ophthalmol Vis Sci 2009;50:2742–2746.
40 Schimmelpfennig BH. Direct and indirect determination of nonuniform cell density distribution in human corneal endothelium. Invest Ophthalmol Vis Sci 1984;25:223–229.
41 Mimura T, Yamagami S, Yokoo S et al. Comparison of rabbit corneal endothelial cell precursors in the central and peripheral cornea. Invest Ophthalmol Vis Sci 2005;46:3645–3648.
42 Garcia MI, Ghiani M, Lefort A et al. LGR5 deficiency deregulates Wnt signaling and leads to precocious Paneth cell differentiation in the fetal intestine. Dev Biol 2009;331:58–67.
43 Schuijers J, Clevers H. Adult mammalian stem cells: the role of Wnt, Lgr5 and R-spondins. EMBO J. 2012.
44 Walker F, Zhang HH, Odorizzi A et al. LGR5 is a negative regulator of tumourigenicity, antagonizes Wnt signalling and regulates cell adhesion in colorectal cancer cell lines. Plos One 2011;6:e22733.

See www.StemCells.com for supporting information available online.

Rho-Associated Kinase Inhibitor Eye Drop Treatment as a Possible Medical Treatment for Fuchs Corneal Dystrophy

Noriko Koizumi, MD, PhD,† Naoki Okumura, MD, PhD,*† Morio Ueno, MD, PhD,* Hiroko Nakagawa, MD,* Junji Hamuro, PhD,* and Shigeru Kinoshita, MD, PhD**

Purpose: To report a case of Fuchs corneal dystrophy that was successfully treated by Rho-associated kinase (ROCK) inhibitor eye drops, subsequent to transcorneal freezing of damaged corneal endothelial cells.

Methods: A 52-year-old Japanese man with a diagnosis of late-onset Fuchs corneal dystrophy was referred to our hospital as a candidate for keratoplasty. Best-corrected vision was 20/20 in the right eye and 20/63 in the left eye. Multiple guttae were observed in both eyes. The right cornea was clear, but the left showed severe central edema, with a central corneal thickness of 703 μm. We were unable to perform specular microscopy in the central cornea, but endothelial cells were observed in the midperiphery at a density of 757 cells per square millimeter. The patient was treated by a corneal endothelial denudation in the prepupillary region followed by the topical administration of a selective ROCK inhibitor, Y-27632, as eye drops for 1 week. Follow-up of 24 months is reported.

Results: Corneal clarity recovered and vision improved to 20/20 two weeks after the treatment. At 6 months, vision had improved to 20/16 and central corneal thickness measured was 568 μm, significantly lower than its pretreatment value. Endothelial function and vision have been well maintained up to the most recent observation, 24 months after the treatment. The average corneal endothelial density in the central and peripheral cornea was 1549.3 ± 89.7 and 705.0 ± 61.1 cells per square millimeter, respectively.

Conclusions: The case highlights the possibility of medical treatments involving the use of ROCK inhibitor eye drops as an alternative to graft surgery for certain forms of corneal endothelial disease.

Key Words: corneal endothelium, medical treatment, Rho kinase inhibitor, Fuchs corneal dystrophy

(*Cornea* 2013;32:1167–1170)

The proliferative ability of human corneal endothelial cells is severely limited in vivo. As a consequence, corneal endothelial damage caused by trauma, intraocular surgery, or disease such as Fuchs corneal dystrophy often results in severe visual disturbance. Corneal transplantation, including corneal endothelial transplantation surgeries such as Descemet stripping automated endothelial keratoplasty (DSAEK) and Descemet membrane endothelial keratoplasty, is a beneficial and realistic treatment for patients with endothelial dysfunction; however, patients will not be totally free from the risk of graft rejection. Moreover, corneal endothelial cell loss is a potential problem in the long-term.[1] Despite the value and potential of endothelial graft surgery, however, a purely pharmacological approach to endothelial recovery remains an attractive proposition.

Previously, we reported that a selective Rho-associated kinase (ROCK) inhibitor, Y-27632, promoted the proliferation of primate corneal endothelial cells in vitro,[2] and the

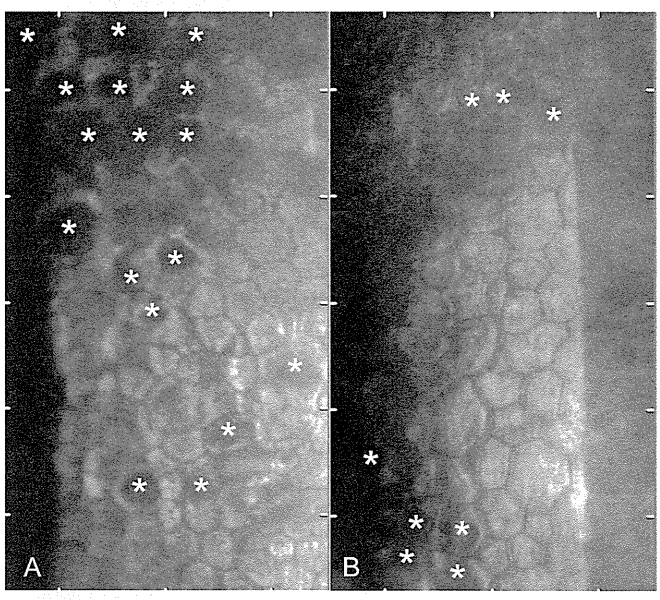

FIGURE 1. The corneal endothelium observed by noncontact specular microscopy before the treatment. A. Multiple guttae were present (*), and corneal endothelial cells at a density of 632 cells per square millimeter were observed in the center of the right cornea. B. We were unable to perform specular microscopy in the center of the left cornea owing to the edema; however, endothelial cells were observed in the midperiphery at a density of 757 cells per square millimeter. Guttae were also observed (*).

Received for publication September 3, 2012; revision received December 21, 2012; accepted December 27, 2012.

From the *Department of Ophthalmology, Kyoto Prefectural University of Medicine, Kyoto, Japan; and †Department of Biomedical Engineering, Faculty of Life and Medical Sciences, Doshisha University, Kyotanabe, Japan.

Supported by A-STEP Feasibility Study from the Japan Science and Technology Agency (AS2314212G for S.K. and N.O.) and the Funding Program for Next Generation World-Leading Researchers from the Cabinet Office in Japan (LS117 for N.K.).

The authors have no funding or conflicts of interest to disclose.

Reprints: Shigeru Kinoshita, Department of Ophthalmology, Kyoto Prefectural University of Medicine, 465 Kajii-cho, Hirokoji-agaru, Kawaramachi-dori, Kamigyo-ku, Kyoto 602-0841, Japan (e-mail: shigeruk@koto.kpu-m.ac.jp).

healing of the corneal endothelium in vivo.[3] Here, we present a case of Fuchs corneal dystrophy scheduled for DSAEK surgery but successfully treated by ROCK inhibitor eye drop treatment subsequent to transcorneal freezing.

CASE REPORT

A 52-year-old Japanese man with blurred vision caused by corneal endothelial dysfunction was referred to the Kyoto Prefectural University of Medicine in May 2008. Visual acuity was 20/20 in the right eye and 20/63 in the left eye. Multiple guttae, typical of Fuchs corneal dystrophy, were observed in both eyes by slit-lamp examination and by noncontact specular microscopy (EM-3000; TOMEY Corporation, Nagoya, Japan) (Figs. 1A, B). The right cornea was clear, although the corneal endothelial density was 632 cells per square millimeter. The left cornea showed severe central edema accompanied by epithelial bullae (Figs. 2A, B). The central corneal thickness was 703 μm in the affected left eye of the patient. We were unable to perform specular microscopy in the central cornea owing to the edema, but endothelial cells were observed in the midperiphery at a density of 757 cells per square millimeter (Fig. 1B). The patient was diagnosed with late-onset Fuchs corneal dystrophy.[4] He was scheduled to have a DSAEK, but in April 2010, he volunteered for an investigative clinical study of a ROCK inhibitor eye drop treatment.

Treatment was initiated on May 18, 2010, according to a protocol approved by the Institutional Review Board of the Kyoto Prefectural University of Medicine. First, diseased corneal endothelium in the prepupillary region was removed by transcorneal freezing[3] by gently pressing a 2-mm-diameter stainless steel rod, which had been cooled in liquid nitrogen onto the corneal surface

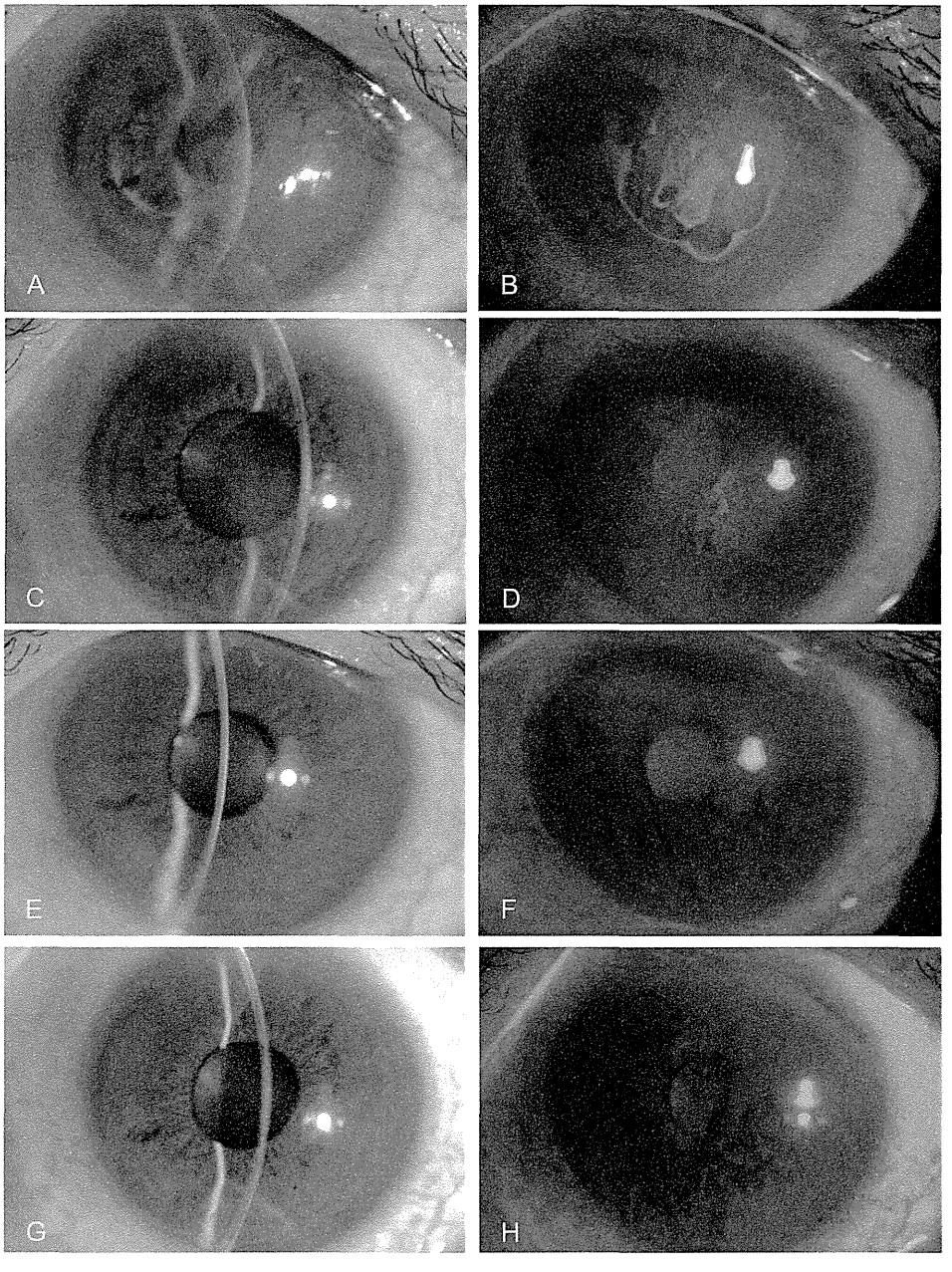

FIGURE 2. Slit-lamp photographs of our Fuchs corneal dystrophy patient before and after transcorneal freezing and ROCK inhibitor treatment. Before treatment, central corneal edema (A) accompanied by a lesion of epithelial bullae (B) was detected. C, D, Three days after the treatment, the corneal erosion created by the transcorneal freezing had already healed, and mild bullae were detected. It should be noted that less corneal edema was observed at 3 days compared with the pretreatment photograph. E, Six months after the treatment, corneal edema was significantly reduced, and cornea had recovered its clarity. F, No epithelial damage was observed by fluorescein staining. G, H, Two years after the treatment, the patient's cornea remains clear with good (20/16) vision.

for 15 seconds. In our previous study using a rabbit model, we confirmed that this transcorneal freezing procedure could make an endothelial defect of approximately the same size as the rod diameter in a reproducible fashion.[3] After the rod was removed and after the cornea had thawed, 50 μL of 10 mM ROCK inhibitor, Y-27632 (Wako, Osaka, Japan), was applied topically as eye drops, repeated 6 times daily for 7 days (May 18–24, 2010). To prevent corneal infection, 0.3% gatifloxacin hydrate eye drops were also applied 4 times daily. Epithelial erosion was detected after transcorneal freezing but had healed by posttreatment day 3 (Figs. 2C, D). No side effects, such as persistent epithelial defects or corneal stromal scars, were observed.

The patient's cornea recovered complete clarity 2 weeks after the treatment, and vision had improved to 20/20. Six months after the treatment, central corneal thickness was 568 μm, significantly lower than its pretreatment value. At this time, vision had improved to 20/16 (Figs. 2E, F). Wide-field endothelial examinations 18 months after the treatment using contact specular microscopy (Konan Medical, Inc, Nishinomiya, Japan; Fig. 3A) showed that the average corneal endothelial densities in the central and peripheral cornea were 1549.3 ± 89.7 and 705 ± 61.1 cells per square millimeter, respectively (mean ± standard error of the mean; Fig. 3B). Although Fuchs corneal dystrophy is a progressive disease, in our patient, corneal clarity and good vision (20/16) have been maintained up to the most recent observation, 2-years after the treatment (Figs. 1G, H).

DISCUSSION

ROCKs are protein serine/threonine kinases, which are the first identified and best-characterized Rho downstream effectors. The Rho/ROCK pathway is involved in regulating the cytoskeleton and has an influence on cell migration, apoptosis, and proliferation.[5–8]

We previously reported that a selective ROCK inhibitor, Y-27632, promoted the proliferation of primate corneal endothelial cells in vitro.[2] In our previous experiments, Y-27632 promoted cell proliferation up to the time when cells became preconfluent but did not promote proliferation in confluent cells whose proliferation had been stopped by contact inhibition. Based on this, and on the results of experiments in rabbits,[3] we hypothesized that the topical application of Y-27632 as an eye drop, combined with the prior partial denudation of diseased corneal endothelial cells, might be useful to promote the proliferation in situ of the corneal endothelium, which is in the early diseased phase. Thus, we came up with the protocol reported here, which shows some potential for the new approach to treat certain types of corneal endothelial dysfunction.

In the posttreatment observation of the presented case, contact specular microscopy revealed relatively small corneal endothelial cells, present at a high cell density, in the central part of cornea from where corneal endothelial cells had been removed by transcorneal freezing. The potential of topical application of ROCK inhibitor suggested by the current report clearly requires a larger comparative study to prove the effect of this new treatment, and plans are underway to conduct this. Regarding the mechanism of action of the procedure, we should also point out that spontaneous remodeling of the human corneal endothelial cells after Descemet stripping has been reported.[9,10] Based on these reports, and also bearing in mind the existence of corneal endothelial precursors with higher proliferative ability in the peripheral cornea,[11,12] we cannot rule out the possibility that reestablishment of this patient's endothelium was not a direct result of ROCK inhibitor administration, but it was the consequence of denudation of the pathologic endothelial cells. Not withstanding the preliminary nature of the current observation, this case report suggests the possibility of a medical treatment for the early phase of diseases, such as Fuchs corneal dystrophy, via the stimulation of nonaffected peripheral cells with ROCK inhibitor after the destruction of diseased cells in the central endothelium by transcorneal freezing.

To the best of our knowledge, this is the first report suggesting that the in vivo proliferation of a patient's corneal endothelium can be stimulated by interventional medical/pharmaceutical treatment after the destruction of diseased

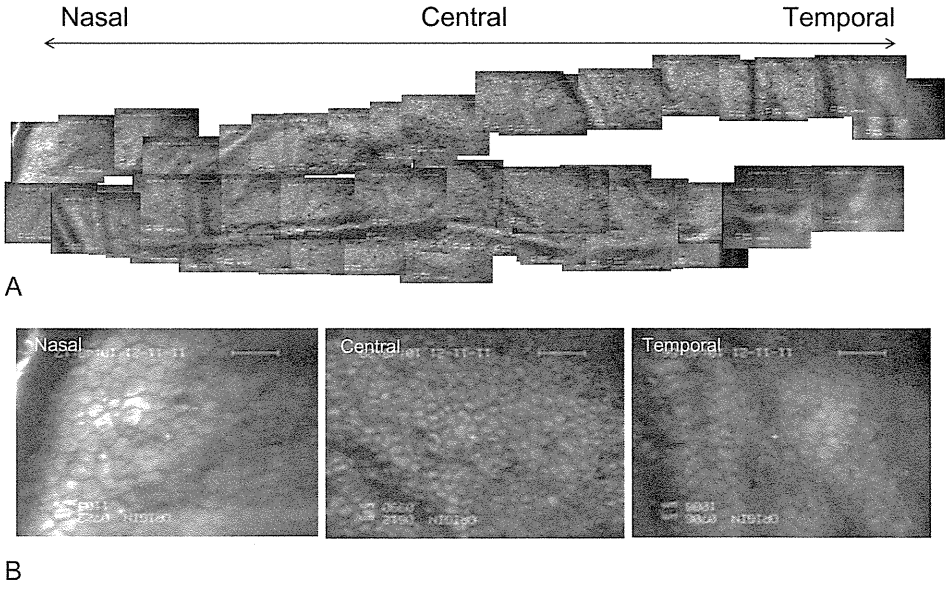

FIGURE 3. A, Wide-field observation of the corneal endothelium by contact-specular microscopy 18 months after the treatment. Guttae were detected mainly in the paracentral area. B, Representative, magnified photographs from nasal peripheral, central, and temporal peripheral area. Smaller cells, present at high density, were observed in the central cornea (scale bar =100 μm).

endothelium. We believe that our new findings will contribute to the opening up of a new approach to the treatment of corneal endothelial dysfunction.

ACKNOWLEDGMENTS

The authors thank Dr. Yoshiki Sasai (RIKEN CDB, Japan) for his invaluable advice regarding ROCK inhibitors and Prof. Andrew Quantock (Cardiff University, United Kingdom) for useful discussions.

REFERENCES

1. Terry MA, Chen ES, Shamie N, et al. Endothelial cell loss after Descemet's stripping endothelial keratoplasty in a large prospective series. *Ophthalmology.* 2008;115:488–496.
2. Okumura N, Ueno M, Koizumi N, et al. Enhancement on primate corneal endothelial cell survival in vitro by a ROCK inhibitor. *Invest Ophthalmol Vis Sci.* 2009;50:3680–3687.
3. Okumura N, Koizumi N, Ueno M, et al. Enhancement of corneal endothelium wound healing by Rho-associated kinase (ROCK) inhibitor eye drops. *Br J Ophthalmol.* 2011;95:1006–1009.
4. Eghrari AO, Gottsch JD. Fuchs' corneal dystrophy. *Expert Rev Ophthalmol.* 2010;5:147–159.
5. Coleman ML, Marshall CJ, Olson MF. RAS and RHO GTPases in G1-phase cell-cycle regulation. *Nat Rev Mol Cell Biol.* 2004;5:355–366.
6. Hall A. Rho GTPases and the actin cytoskeleton. *Science* 1998;279: 509–514.
7. Olson MF, Ashworth A, Hall A. An essential role for Rho, Rac, and Cdc42 GTPases in cell cycle progression through G1. *Science.* 1995;269: 1270–1272.
8. Watanabe K, Ueno M, Kamiya D, et al. A ROCK inhibitor permits survival of dissociated human embryonic stem cells. *Nat Biotechnol.* 2007;25:681–686.
9. Balachandran C, Ham L, Verschoor CA, et al. Spontaneous corneal clearance despite graft detachment in Descemet membrane endothelial keratoplasty. *Am J Ophthalmol.* 2009;148:227–234.
10. Shah RD, Randleman JB, Grossniklaus HE. Spontaneous corneal clearing after Descemet's stripping without endothelial replacement. *Ophthalmology.* 2012;119:256–260.
11. Mimura T, Joyce N. Replication competence and senescence in central and peripheral human corneal endothelium. *Invest Ophthalmol Vis Sci.* 2006;47:1387–1396.
12. Mimura T, Yamagami S, Yokoo S, et al. Comparison of rabbit corneal endothelial cell precursors in the central and peripheral cornea. *Invest Ophthalmol Vis Sci.* 2005;46:3645–3648.

PLOS ONE

Inhibition of TGF-β Signaling Enables Human Corneal Endothelial Cell Expansion *In Vitro* for Use in Regenerative Medicine

Naoki Okumura[1,2], EunDuck P. Kay[1], Makiko Nakahara[1], Junji Hamuro[2], Shigeru Kinoshita[2], Noriko Koizumi[1]*

1 Department of Biomedical Engineering, Faculty of Life and Medical Sciences, Doshisha University, Kyotanabe, Japan, **2** Department of Ophthalmology, Kyoto Prefectural University of Medicine, Kyoto, Japan

Abstract

Corneal endothelial dysfunctions occurring in patients with Fuchs' endothelial corneal dystrophy, pseudoexfoliation syndrome, corneal endotheliitis, and surgically induced corneal endothelial damage cause blindness due to the loss of endothelial function that maintains corneal transparency. Transplantation of cultivated corneal endothelial cells (CECs) has been researched to repair endothelial dysfunction in animal models, though the *in vitro* expansion of human CECs (HCECs) is a pivotal practical issue. In this study we established an optimum condition for the cultivation of HCECs. When exposed to culture conditions, both primate and human CECs showed two distinct phenotypes: contact-inhibited polygonal monolayer and fibroblastic phenotypes. The use of SB431542, a selective inhibitor of the transforming growth factor-beta (TGF-β) receptor, counteracted the fibroblastic phenotypes to the normal contact-inhibited monolayer, and these polygonal cells maintained endothelial physiological functions. Expression of ZO-1 and Na^+/K^+-ATPase maintained their subcellular localization at the plasma membrane. Furthermore, expression of type I collagen and fibronectin was greatly reduced. This present study may prove to be the substantial protocol to provide the efficient *in vitro* expansion of HCECs with an inhibitor to the TGF-β receptor, and may ultimately provide clinicians with a new therapeutic modality in regenerative medicine for the treatment of corneal endothelial dysfunctions.

Citation: Okumura N, Kay EP, Nakahara M, Hamuro J, Kinoshita S, et al. (2013) Inhibition of TGF-β Signaling Enables Human Corneal Endothelial Cell Expansion *In Vitro* for Use in Regenerative Medicine. PLoS ONE 8(2): e58000. doi:10.1371/journal.pone.0058000

Editor: Che John Connon, University of Reading, United Kingdom

Received November 5, 2012; **Accepted** January 29, 2013; **Published** February 25, 2013

Funding: The work was supported in part by the Highway Program for realization of regenerative medicine (Kinoshita and Okumura); http://www.mext.go.jp/english/; and the Funding Program for Next Generation World-Leading Researchers from the Cabinet Office in Japan (Koizumi: LS117); http://www.jsps.go.jp/english/e-jisedai/index.html. The funders had no role in study design, data collection and analysis, decision to publish, or preparation of the manuscript.

Competing Interests: The authors have declared that no competing interests exist.

* E-mail: nkoizumi@mail.doshisha.ac.jp

Introduction

Corneal endothelial dysfunction is a major cause of severe visual impairment leading to blindness due to the loss of endothelial function that maintains corneal transparency. Restoration to clear vision requires either full-thickness corneal transplantation or endothelial keratoplasty. Recently, highly effective surgical techniques to replace corneal endothelium [e.g., Descemet's stripping automated endothelial keratoplasty (DSAEK) and Descemet's membrane endothelial keratoplasty (DMEK)] have been developed [1–3] that are aimed at replacing penetrating keratoplasty for overcoming pathological dysfunctions of corneal endothelial tissue. At present, our group and several other research groups have focused on the establishment of new treatment methods suitable for a practical clinical intervention to repair corneal endothelial dysfunctions [4–9]. Since corneal endothelium is composed of a monolayer and is a structurally flexible cell sheet, corneal endothelial cells (CECs) have been cultured on substrates including collagen sheets, amniotic membrane, or human corneal stroma. Then the cultured CECs are transplanted as a cell sheet. However, these techniques require the use of an artificial or biological substrate that may introduce several problems such as substrate transparency, detachment of the cell sheet from the cornea, and technical difficulty of transplantation into the anterior chamber. In our effort to overcome those substrate-related problems, we previously demonstrated that the transplantation of cultivated CECs in combination with a Rho kinase (ROCK) inhibitor enhanced the adhesion of injected cells onto the recipient corneal tissue without the use of a substrate and successfully achieved the recovery of corneal transparency in two corneal-endothelial-dysfunction animal models (rabbit and primate) [10,11].

However, in the context of the clinical setting, another pivotal practical issue is the *in vitro* expansion of human CECs (HCECs). HCECs are vulnerable to morphological fibroblastic change under normal culture conditions. Although HCECs can be cultivated into a normal phenotype maintaining the contact-inhibited polygonal monolayer, they eventually undergo massive endothelial-mesenchymal transformation after long-term culture or subculture. Thus, cultivation of HCECs with normal physiological function is difficult, yet not impossible [12,13].

Epithelial mesenchymal transformation (EMT) has been well characterized in epithelial-to-mesenchymal transition, and transforming growth factor-beta (TGF-β) can initiate and maintain EMT in a variety of biological and pathological systems [14,15].

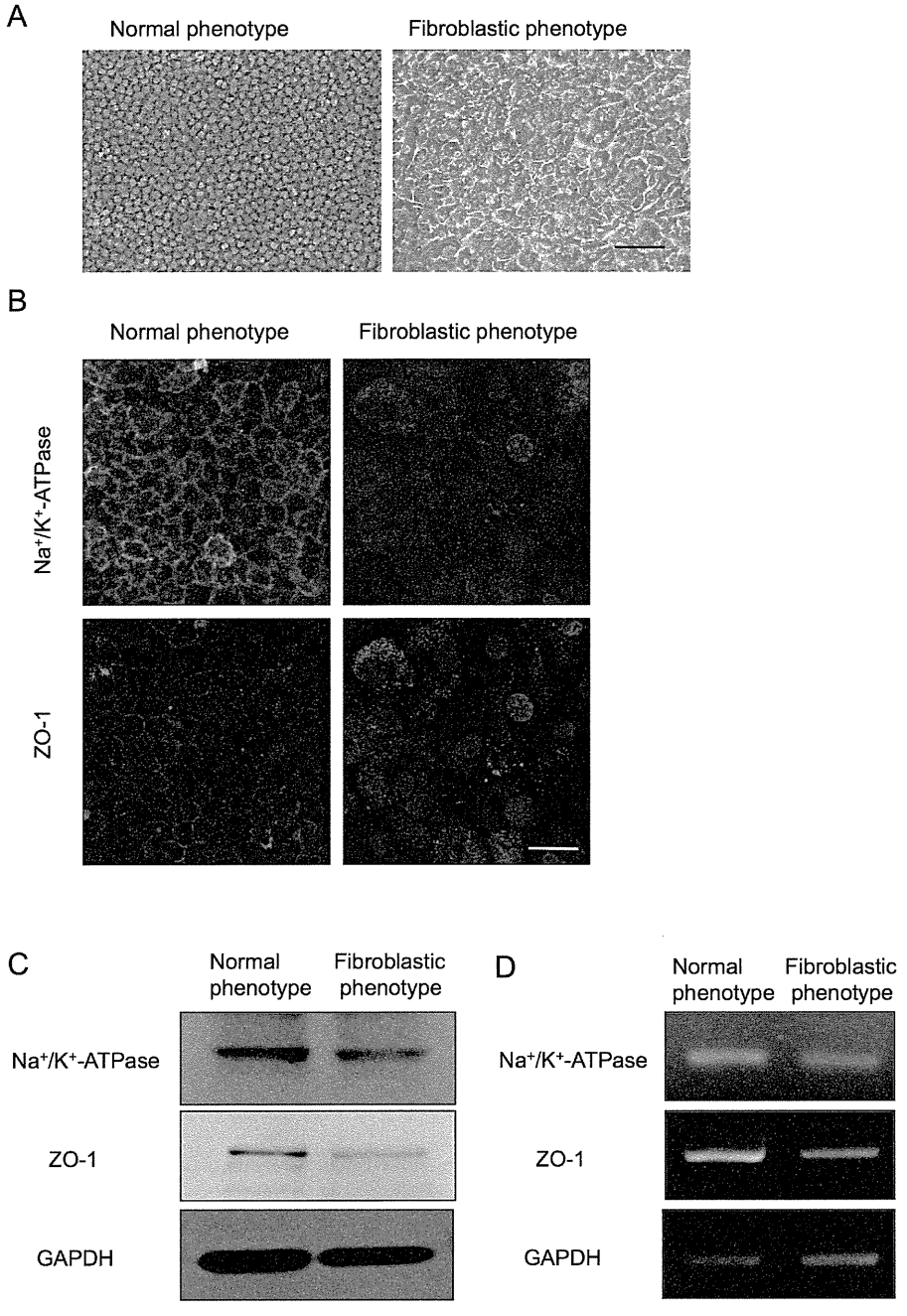

Figure 1. Primate corneal endothelial cells exhibit fibroblastic phenotype and lose functions during cell culture. (A) Cultivated primate CECs demonstrated two distinctive phenotypes; the cells maintained the characteristic polygonal cell morphology and contact-inhibited phenotype (normal phenotype) and the cells showed a fibroblastic cell shape with multi-layering (fibroblastic phenotype). Both phenotypes of the cultured CECs were primary cultured cells. Scale bar: 50 μm. The experiment was performed in triplicate. (B) Na^+/K^+-ATPase and ZO-1 at the plasma membrane was preserved in the normal phenotype, while fibroblastic phenotype completely lost the characteristic staining profile of Na^+/K^+-ATPase and ZO-1 at the plasma membrane. Scale bar: 100 μm. (C+D) Expression of the Na^+/K^+-ATPase and ZO-1 was higher in normal phenotypes than in the fibroblastic phenotypes at both the protein and mRNA levels. Samples were prepared in duplicate. Immunoblotting and semiquantitative PCR were performed in duplicate.
doi:10.1371/journal.pone.0058000.g001

The cellular activity of TGF-β is of particular interest in epithelial cells, as it inhibits the G1/S transition of the cell cycle in these cells. However, the same growth factor is the key signaling molecule for EMT, and the role of TGF-β as a key molecule in the development and progression of EMT is well studied [14–17]. Smad2/3 are signaling molecules downstream of cell-surface receptors for TGF-β in epithelial-to-mesenchymal transition [16,17]. Similar to epithelial cells, TGF-β inhibits the G1/S transition of the cell cycle in CECs [18,19], however, it is not known how TGF-β develops endothelial to mesenchymal transformation and maintains it in CECs. Endothelial-mesenchymal transformation is observed among corneal endothelial dysfunctions such as Fuchs' endothelial corneal dystrophy, pseudoexfoliation syndrome, corneal endotheliitis, surgically-induced corneal

endothelial damage, and corneal trauma and it induces the fibroblastic transformation of CECs [20–23], suggesting that CECs have the biological potential to acquire endothelial to mesenchymal transformation. The apparent presence of fibroblastic phenotypes in primate CECs and HCECs in culture led us to search for the cause of such phenotypic changes of the cultivated cells and for a means in which to prevent such undesirable cellular changes toward endothelial-mesenchymal transformation.

In the present study, we established primate CEC and HCEC cultures which respectively showed two distinctive phenotypes: 1) normal and 2) fibroblastic. We further characterized the two phenotypes and showed evidence that the use of an inhibitor to TGF-β receptor or BMP-7 abolished the fibroblastic phenotypes of cultivated CECs. Thus, intervention by inhibiting the endothelial to mesenchymal transformation process that occurs during the cultivation of CECs will certainly enable the *in vitro* expansion of cultivated HCECs with a normal phenotype which would be ideal for therapeutic clinical application.

Materials and Methods

Ethics Statement

The monkey tissue used in this study was handled in accordance with the ARVO Statement for the Use of Animals in Ophthalmic and Vision Research. The isolation of the tissue was approved by an institutional animal care and use committee of the Nissei Bilis Co., Ltd. (Otsu, Japan) and the Eve Bioscience, Co., Ltd. (Hashimoto, Japan). The human tissue used in this study was handled in accordance with the tenets set forth in the Declaration of Helsinki. A written consent was acquired from the next of kin of all deceased donors regarding eye donation for research. All tissue is recovered under the tenants of the Uniform Anatomical Gift Act (UAGA) of the particular state where the donor was consented and recovered.

Monkey cornea tissues and Research-grade human cornea tissues

Eight corneas from 4 cynomolgus monkeys (3 to 5 years-of-age; estimated equivalent human age: 5 to 20 years) housed at Nissei Bilis and the Keari Co., Ltd., Osaka, Japan, respectively, were used for the MCECs culture. The cynomolgus monkeys were housed in individual stainless steel cages at Nissei Bilis and Eve Bioscience. Each cage was provided with reverse-osmosis water delivered by an automatic water supply system and supplied with experimental animal diet (PS-A; Oriental Yeast Co., Ltd., Tokyo, Japan). Room temperature was controlled by heating units inside the rooms and was maintained at 18.0–26.0°C. The humidity was maintained at 29.5 to 80.4%. Animals were maintained on a 12:12-h light:dark cycle (lights on, 7 a.m. to 19 p.m.). For other research purposes, the animals were given an overdose of intravenous pentobarbital sodium for euthanatization. The corneas of cynomolgus monkeys were harvested after confirmation of cardiopulmonary arrest by veterinarians, and then provided for our research. Twenty human donor corneas were obtained from the SightLife™ (Seattle, WA) eye bank, and all corneas were stored at 4°C in storage medium (Optisol; Chiron Vision Corporation, Irvine, CA) for less than 14 days prior to the primary culture.

Cell culture of monkey CECs (MCECs)

The MCECs were cultivated in modified protocol as described previously [7,24]. Briefly, the Descemet's membrane including CECs was stripped and digested at 37°C for 2 h with 1 mg/mL collagenase A (Roche Applied Science, Penzberg, Germany). After a digestion at 37°C, the MCECs obtained from individual corneas were resuspended in culture medium and plated in 1 well of a 6-well plate coated with FNC Coating Mix® (Athena Environmental

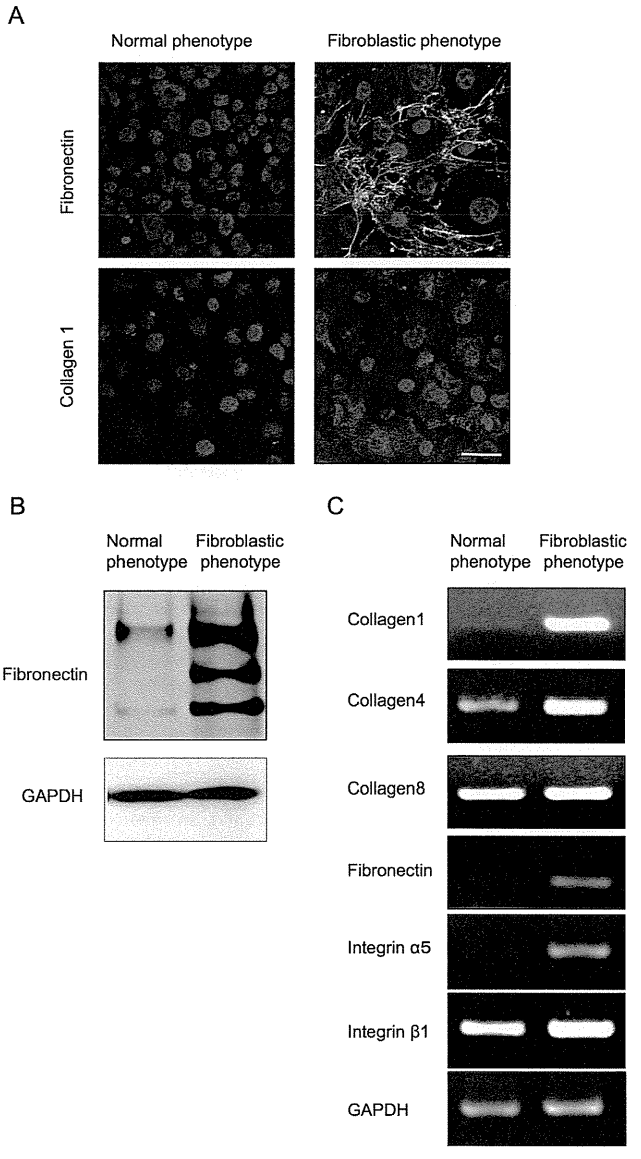

Figure 2. Fibroblastic primate CECs produced an abnormal extra cellular matrix. (A) The fibroblastic phenotype demonstrated excessive ECMs such as fibronectin and collagen type 1, while the normal phenotype completely lost the staining potential. Scale bar: 100 μm. (B) The protein expression level of fibronectin was more strongly upregulated in the fibroblastic phenotype than in the normal phenotype. (C) Semiquantitative PCR analysis showed that the type I collagen transcript [α1(I) mRNA] was abundantly expressed in the fibroblastic phenotypes, while the expression of α1(I) mRNA was reduced in the normal phenotypes. The basement membrane collagen phenotype α1(IV) mRNA was expressed both in normal and fibroblastic phenotypes, yet to a lesser degree in the normal phenotype. Collagen phenotype α1(VIII) mRNA was expressed in both phenotypes at similar levels. Fibronectin and integrin α5 mRNA was observed in the fibroblastic phenotypes, as opposed to the normal phenotypes in which the two transcripts were not expressed. β1 integrin mRNA was expressed in both phenotypes at similar levels. Samples were prepared in duplicate. Immunoblotting and semiquantitative PCR were performed in duplicate.
doi:10.1371/journal.pone.0058000.g002

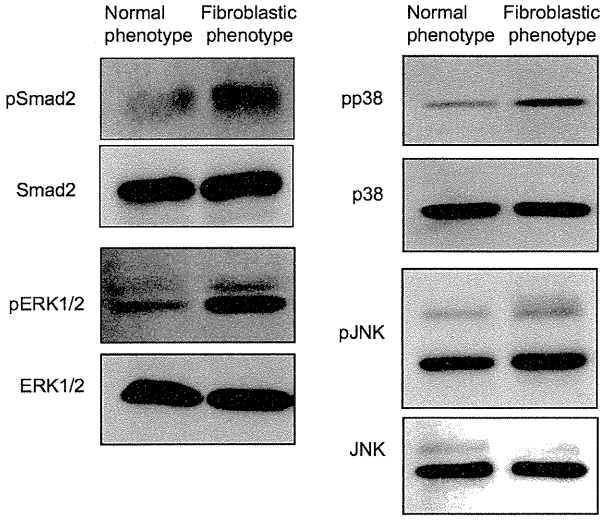

Figure 3. Different activation pattern of fibroblastic change associated pathways in the fibroblastic phenotype of primate CECs. Phosphorylation of Smad2, p38MAPK, and ERK1/2 was promoted in the fibroblastic phenotype compared to that in the normal phenotype, while phosphorylation of JNK was negligible. Samples were prepared in duplicate, and immunoblotting was performed in duplicate.
doi:10.1371/journal.pone.0058000.g003

Sciences, Inc., Baltimore, MD). All primary cell cultures and serial passages of the MCECs were performed in growth medium composed of Dulbecco's modified Eagle's medium (Invitrogen Corporation, Carlsbad, CA) supplemented with 10% fetal bovine serum (FBS), 50 U/mL penicillin, 50 μg/mL streptomycin, and 2 ng/mL FGF-2 (Invitrogen). The MCECs were then cultured in a humidified atmosphere at 37°C in 5% CO_2, and the culture medium was changed every 2 days. When the MCECs reached confluency in 10 to 14 days, they were rinsed in Ca^{2+} and Mg^{2+}-free Dulbecco's phosphate-buffered saline (PBS), trypsinized with 0.05% Trypsin-EDTA (Invitrogen) for 5 min at 37°C, and passaged at ratios of 1:2–4. Cultivated MCECs at passages 2 through 5 were used for all experiments. SB431542 (Merck Millipore, Billerica, MA), a selective inhibitor of transforming growth factor-β (TGF-beta), was tested for the anti-fibroblastic effect.

Cell culture of HCECs

The HCECs were cultivated in a modified version of the protocol used for the MCECs. Briefly, the Descemet's membrane including CECs was stripped and digested at 37°C for 2 h with 1 mg/mL collagenase A (Roche Applied Science). After a digestion at 37°C, the HCECs obtained from individual corneas were resuspended in culture medium and plated in 1 well of a 12-well plate coated with FNC Coating Mix®. The culture medium was prepared according to published protocols [25], but with some modifications. Briefly, basal culture medium containing Opti-MEM-I (Invitrogen), 8% FBS, 5 ng/mL epidermal growth factor (EGF) (Sigma-Aldrich Co., St. Louis, MO), 20 μg/mL ascorbic acid (Sigma-Aldrich), 200 mg/L calcium chloride (Sigma-Aldrich), 0.08% chondroitin sulfate (Wako Pure Chemical Industries, Ltd., Osaka, Japan), and 50 μg/mL of gentamicin was prepared, and the conditioned medium was then recovered after cultivation of inactivated 3T3 fibroblasts. Inactivation of the 3T3 fibroblasts was performed as described previously [26,27]. Briefly, confluent 3T3 fibroblasts were incubated with 4 μg/mL mitomycin C (MMC) (Kyowa Hakkko Kirin Co., Ltd., Tokyo, Japan) for 2 h at 37°C under 5% CO_2, and then trypsinized and plated onto plastic dishes at the density of 2×10^4 cells/cm^2. The HCECs were cultured in a humidified atmosphere at 37°C in 5% CO_2, and the culture medium was changed every 2 days. When the HCECs reached confluency in 14 to 28 days, they were rinsed in Ca^{2+} and Mg^{2+}-free PBS, trypsinized with 0.05% Trypsin-EDTA for 5 min at 37°C, and passaged at ratios of 1:2. Cultivated HCECs at passages 2 through 5 were used for all experiments. To test the anti-fibroblastic effect, the cultured HCECs were passaged at the ratio of 1:2 with medium supplemented with or without SB431542 (0.1, 1, and 10 μM) (Merck Millipore), a neutralizing antibody to TGF-β (500 ng/ml) (R&D Systems, Inc., Minneapolis, MN), Smad3 inhibitor (3 mM) (Merck Millipore), and bone morphogenetic protein (BMP) BMP-7 (10, 100, and 1000 ng/ml) (R&D Systems), and were then evaluated after 1 week.

Histological examination

For histological examination, cultured MCECs or HCECs on Lab-Tek™ Chamber Slides™ (NUNC A/S, Roskilde, Denmark) were fixed in 4% formaldehyde for 10 min at room temperature (RT) and incubated for 30 min with 1% bovine serum albumin (BSA). To investigate the phenotype of the CECs, immunohistochemical analyses of ZO-1 (Zymed Laboratories, Inc., South San Francisco, CA), a tight junction associated protein, Na^+/K^+-ATPase (Upstate Biotechnology, Inc., Lake Placid, NY), the protein associated with pump function, fibronectin (BD, Franklin Lakes, NJ), and actin were performed. ZO-1 and Na^+/K^+-ATPase were used as function related markers of the CECs, fibronectin and collagen type 1 were used to evaluate the fibroblastic change, and actin staining was used to evaluate the cellular morphology. The ZO-1, Na^+/K^+-ATPase, collagen type 1, and fibronectin staining were performed with a 1:200 dilution of ZO-1 polyclonal antibody, Na^+/K^+-ATPase monoclonal antibody, and fibronectin monoclonal antibody, respectively. For the secondary antibody, a 1:2000 dilution of Alexa Fluor® 488-conjugated or Alexa Fluor® 594-conjugated goat anti-mouse IgG (Invitrogen) was used. Actin staining was performed with a 1:400 dilution of Alexa Fluor® 488-conjugated phalloidin (Invitrogen). Cell nuclei were then stained with DAPI (Vector Laboratories, Inc., Burlingame, CA) or propidium iodide (PI) (Sigma-Aldrich). The slides were then inspected by fluorescence microscopy (TCS SP2 AOBS; Leica Microsystems, Wetzlar, Germany). The percentages of Na^+/K^+-ATPase- and ZO-1-positive cells that expressed Na^+/K^+-ATPase and ZO-1 at the plasma membrane in the *in vivo* condition were counted by a blinded examiner.

Immunoblotting

For immunoblotting, the cells were washed with PBS and then lysed with radio immunoprecipitation assay (RIPA) buffer (Bio-Rad Laboratories, Hercules, CA) containing Phosphatase Inhibitor Cocktail 2 (Sigma-Aldrich) and Protease Inhibitor Cocktail (Nacalai Tesque, Kyoto, Japan). The lysates were then centrifuged at 15,000 rpm for 10 min at 4°C. The resultant supernatant was collected and the protein concentration of the sample was assessed with the BCA™ Protein Assay Kit (Takara Bio Inc., Otsu, Japan). The proteins were then separated by sodium dodecyl sulfate polyacrylamide gel electrophoresis (SDS-PAGE) and transferred to polyvinylidene fluoride (PVDF) membranes. The membranes were then blocked with 3% non-fat dry milk (Cell Signaling Technology, Inc., Danvers, MA) in TBS-T buffer. The incubations were then performed with the following primary antibodies: Na^+/K^+-ATPase (Merck Millipore), ZO-1, GAPDH (Abcam, Cambridge, UK), fibronectin, and Smad2 (Cell Signaling Technology),

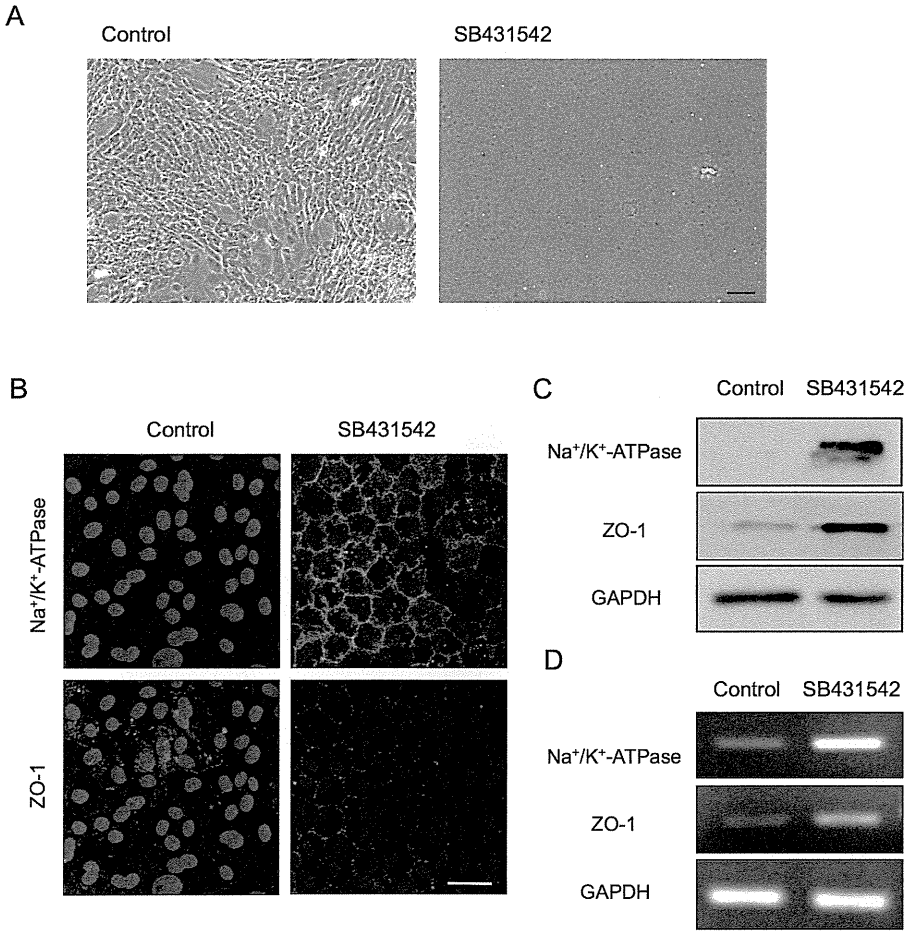

Figure 4. Inhibition of the TGF-β pathway suppressed fibroblastic change and maintained functions. (A) Primate CECs cultured with SB431542 exhibited the authentic polygonal cell shape and contact-inhibited monolayer, while the control CECs exhibited the fibroblastic morphology. Scale bar: 50 μm. (B) SB431542-treated CECs showed the characteristic plasma membrane staining of Na^+/K^+-ATPase and ZO-1, while the control CECs lost their staining. Scale bar: 100 μm. (C+D) Expression of Na^+/K^+-ATPase and ZO-1 was greatly upregulated in the SB431542-treated fibroblastic phenotypes at both the protein and mRNA levels. Samples were prepared in duplicate. Immunoblotting and semiquantitative PCR were performed in duplicate.
doi:10.1371/journal.pone.0058000.g004

phosphorylated Smad2 (Cell Signaling Technology), ERK1/2 (BD), phosphorylated ERK1/2 (BD), p38MAPK (BD), phosphorylated p38MAPK (BD) JNK (BD) or phosphorylated JNK (BD) (1:1000 dilution), and HRP-conjugated anti-rabbit or anti-rabbit IgG secondary antibody (Cell Signaling Technology) (1:5000 dilution). Membranes were exposed by ECL Advance Western Blotting Detection Kit (GE Healthcare, Piscataway, NJ), and then examined by use of the LAS4000S (Fujifilm, Tokyo, Japan) imaging system.

Semiquantitative reverse transcriptase polymerase chain reaction (RT-PCR) and quantitative PCR

Total RNA was extracted from CECs and cDNA was synthesized by use of ReverTra Ace® (Toyobo, Osaka, Japan), a highly efficient RT. The same amount of cDNA was amplified by PCR (GeneAmp 9700; Applied Biosystems) and the following primer pairs: GAPDH mRNA, forward (5′-GAGTCAACGGATTTGGTCGT-3′), and reverse (5′-TTGATTTTGGAGGGATCTCG-3′); Na^+/K^+-ATPase mRNA, forward (5′-CTTCCTCCGCATTTATGCTCATTTTCTCACCC-3′), and reverse (5′-GGATGATCATAAACTTAGCCTTGATGAACTC-3′); ZO-1 mRNA, forward (5′-GGACGAGGCATCATCCCTAA-3′), and reverse (5′-CCAGCTTCTCGAAGAACCAC-3′); collagen1 mRNA, forward (5′-TCGGCGAGAGCATGACCGATGGAT-3′), and reverse (5′-GACGCTGTAGGT GAAGCGGCTGTT-3′); collagen4 mRNA, forward (5′-AGCAAGGTGTTACAGGATTGGT -3′), and reverse (5′- AGAAGGACACTGTGGGTCATCT -3′); collagen8 mRNA, forward (5′-ATGTGATGGCTGTGCTGCTGCTGCCT -3′), and reverse (5′-CTCTTGGGCCAGGCTCTCCA-3′); fibronectin mRNA, forward (5′-AGATGAGTGGGAACGAATGTCT -3′), and reverse (5′-GAGGGTCACACTTGAATTCTCC -3′); integrin α5 mRNA, forward (5′-TCCTCAGCAAGAATCTCAACAA -3′), and reverse (5′-GTTGAGTCCCGTAACTCTGGTC -3′); integrin β1 mRNA, forward (5′-GCTGAAGACTATCCCATTGACC -3′), and reverse (5′-ATTTCCAGATATGCGCTGTTTT -3′). PCR products were analyzed by agarose gel electrophoresis. Quantitative PCR was performed using the following TaqMan® (Invitrogen) primers: collegen1, Hs00164004_m1; fibronectin, Hs01549976_m1; GAPDH, Hs00266705_g1. The PCR was performed using the StepOne™ (Applied Biosystems) real-time PCR system. GAPDH was used as an internal standard.

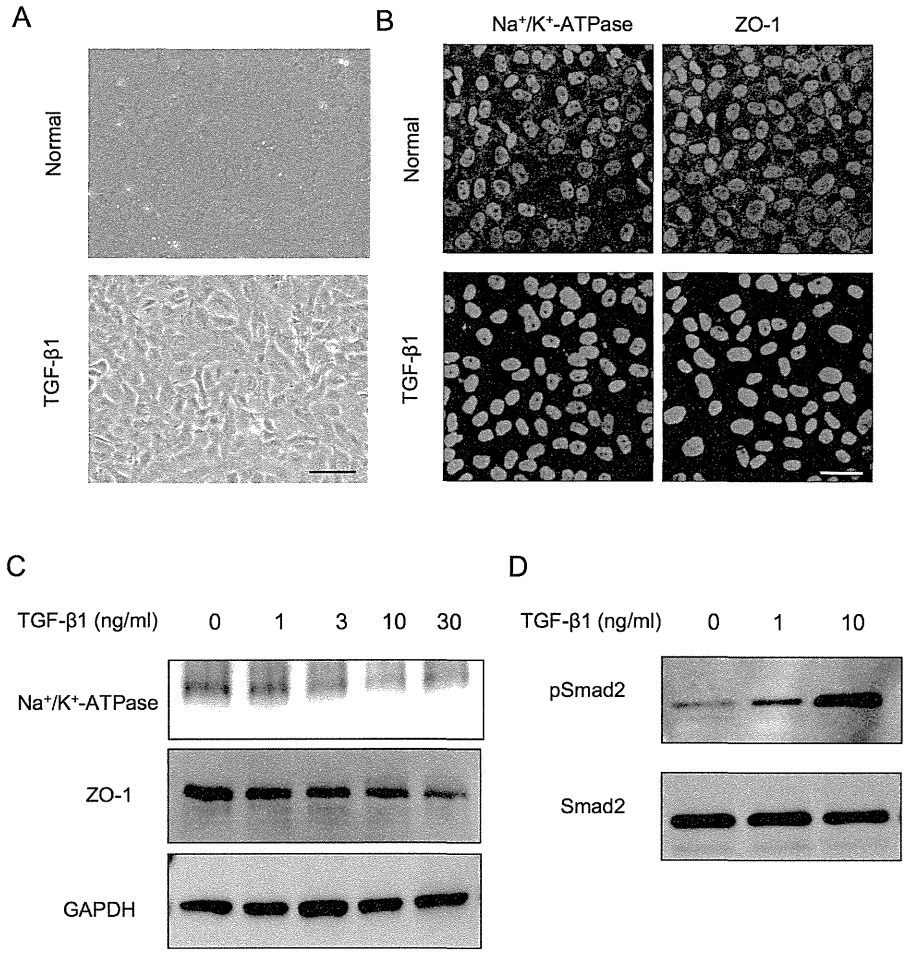

Figure 5. TGFβ induced fibroblastic change and function loss through the activation of the Smad signaling pathways. (A) Normal phenotype primate CECs were transformed to fibroblastic cells when exposed to the exogenous TGF-β1 (10 ng/ml). Scale bar: 50 μm. (B) The staining pattern of Na^+/K^+-ATPase and ZO-1 at the plasma membrane of the normal phenotypes was greatly reduced upon exposure to TGF-β1 (10 ng/ml). Scale bar: 100 μm. (C) TGF-β1 reduced the expression of Na^+/K^+-ATPase and ZO-1 at protein levels dose-dependently. (D) Phosphorylation of Smad2 was increased in a concentration-dependent manner. Samples were prepared in duplicate, and immunoblotting was performed in duplicate.
doi:10.1371/journal.pone.0058000.g005

Enzyme-linked immunosorbent assay (ELISA)

Collagen type I of culture medium supernatant of HCECs were measured using ELISA kits for Collagen Type I Alpha 2 (COL1a2) (Uscn Life Science Inc., Wuhan, China) according to the manufacturer's instructions. Culture medium supernatant from HCECs cultured with or without SB431542 were used for each group (n = 5).

Statistical analysis

The statistical significance (*P*-value) in mean values of the two-sample comparison was determined by use of the Student's t-test. The statistical significance in the comparison of multiple sample sets was analyzed by use of the Dunnett's multiple-comparisons test. Values shown on the graphs represent the mean ± SE.

Results

Two distinct phenotypes of primate CECs during cell culture

Of great interest, the primate CECs in culture demonstrated two distinctive phenotypes when determined by cell morphology and the characteristic contact-inhibited phenotype. Although to culture primate CECs in a normal phenotype while maintaining the monolayer contact-inhibited morphology is possible, they often showed morphological fibroblastic change after primary culture following isolation from the cornea, or long-term culture or subculture, if they were once primary cultured in normal morphology (Fig. 1A). The two phenotypes were then tested for the endothelial characteristics; the staining pattern of Na^+/K^+-ATPase and ZO-1 at the plasma membrane was well preserved in the normal phenotypes, yet the fibroblastic phenotypes completely lost the characteristic staining profile of Na^+/K^+-ATPase and ZO-1 at the plasma membrane (Fig. 1B). Expression of the two functional proteins was found to be much greater in the normal phenotypes than in the fibroblastic phenotypes at both the protein (Fig. 1C) and mRNA levels (Fig. 1D). Comparison of the expression of authentic fibrillar extracellular matrix (ECM) proteins showed that fibroblastic phenotypes demonstrated a fibrillar ECM staining pattern of fibronectin, while the normal phenotypes completely lost the staining potential of fibronectin (Fig. 2A). The protein expression level of fibronectin was more strongly upregulated in the fibroblastic phenotypes than in the normal phenotypes (Fig. 2B). Type I collagen produced by fibroblastic phenotypes demonstrated dual locations, at the ECM

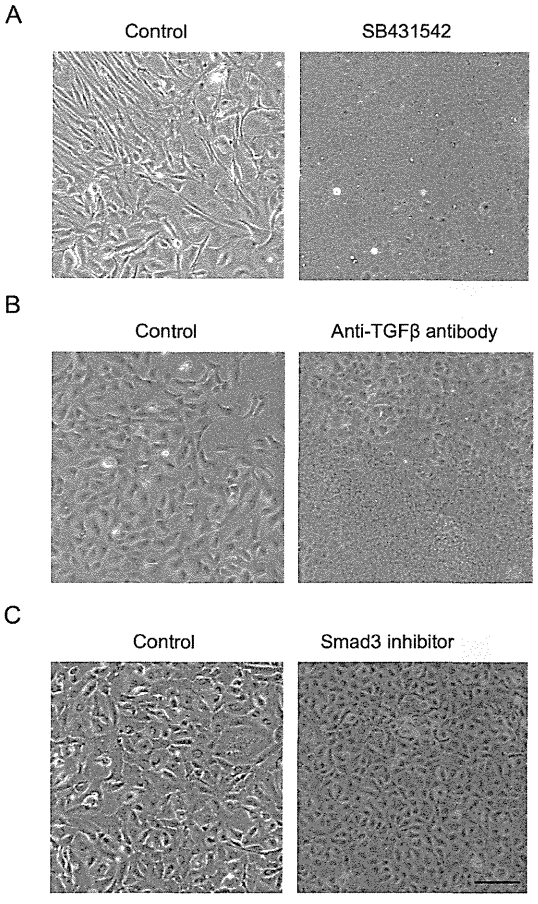

Figure 6. Inhibition of the TGFβ pathway suppressed the fibroblastic change of HCECs. (A) HCECs cultured with SB431542 (1 μM) exhibited the hexagonal cell shape and contact-inhibited monolayer, while the control CECs exhibited the fibroblastic morphology. (B+C) Both neutralizing antibody to TGF-β (500 ng/ml) and Smad3 inhibitor (3 mM) blocked cells from acquiring fibroblastic phenotypes. Scale bar: 50 μm. The experiment was performed in duplicate.
doi:10.1371/journal.pone.0058000.g006

and at the cytoplasm. Of interest, the cytoplasmic location of type I collagen appeared to be at the Golgi complex, the intracellular localization of which is essential for secretion, and these findings are similar to the published data [28]. On the other hand, type I collagen staining in the normal phenotypes was not clearly observed (Fig. 2A). RT-PCR analysis was used to determine the expression of major ECM proteins. The type I collagen transcript [α1(I) mRNA] was found to be abundantly expressed in the fibroblastic phenotypes, while the expression of α1(I) mRNA was negligible in the normal phenotypes (Fig. 2C). Unlike the type I collagen transcript, the basement membrane collagen phenotype α1(IV) mRNA was expressed in both the normal and fibroblastic phenotypes, yet to a lesser degree in the normal phenotype. Collagen phenotype α1(VIII) mRNA was expressed in both phenotypes at similar levels. Expression of fibronectin and integrin α5 was observed in the fibroblastic phenotypes, as opposed to the normal phenotypes in which the two transcripts were not expressed (Fig. 2C). On the other hand, β1 integrin mRNA was expressed in both phenotypes at similar levels (Fig. 2C).

Next, signaling pathways were determined to elucidate what might cause fibroblastic phenotypes of CECs. Since Smad2, p38, ERK1/2, and JNK are reportedly all involved in the EMT pathway [18–20,29,30], we therefore tested whether Smad2 and the MAPKs were involved in an endothelial-mesenchymal transformation similar to the EMT observed in epithelial cells (Fig. 3). Phosphorylation of Smad2 was found to be greatly promoted in the fibroblastic phenotypes when compared to that in the normal phenotypes. Phosphorylation of p38 and ERK1/2 was greatly enhanced in the fibroblastic phenotypes, while activation of JNK was negligible. These findings suggested that TGF-β signaling may exert the key role for the fibroblastic transformation of CECs.

TGF-β-mediated endothelial-mesenchymal transformation and use of TGF-β receptor inhibitor to block it in primate CECs

The findings shown in Fig. 3 led us to directly test whether SB431542, the TGF-β receptor inhibitor, was able to block the EMT process observed in the fibroblastic phenotypes. Phase contrast imaging demonstrated that primate CECs cultured in the presence of SB431542 exhibited the authentic polygonal cell shape and contact-inhibited monolayer, while the control CECs exhibited the fibroblastic morphology (Fig. 4A). Moreover, the SB431542-treated CECs showed the characteristic plasma membrane staining of Na^+/K^+-ATPase and ZO-1, while the control CECs lost their staining, suggesting that endothelial functions were maintained in the SB431542-treated cells (Fig. 4B). Furthermore, the expression of Na^+/K^+-ATPase and ZO-1 was strongly upregulated in the SB431542-treated fibroblastic phenotypes at both the protein (Fig. 4C) and mRNA levels (Fig. 4D). These data further confirmed that TGF-β might be the direct mediator of the endothelial to mesenchymal transformation observed in primate CEC cultures. Therefore, we tested whether the normal phenotypes were transformed to fibroblastic cells when exposed to the exogenous TGF-β, as in the findings shown in Fig. 5A. Of interest, the staining pattern of Na^+/K^+-ATPase and ZO-1 at the plasma membrane of the normal phenotypes was greatly reduced upon exposure of polygonal cells to TGF-β (Fig. 5B). The growth factor also markedly reduced the expression of the two proteins at protein levels in a concentration-dependent manner (Fig. 5C), while phosphorylation of Smad2 was greatly increased in a concentration-dependent manner (Fig. 5D). These data suggest that even the normal phenotypes of primate CECs are prone to acquire fibroblastic phenotypes in response to TGF-β-stimulation.

Two distinct phenotypes of HCEC cultures and the use of TGF-β receptor inhibitor to block endothelial-mesenchymal transformation

The interesting findings observed in primate CECs led us to further study whether HCECs were subjected to the similar undesirable prerequisite cellular changes leading to endothelial-mesenchymal transformation. Of great interest, cultivated HCECs lost the characteristic contact-inhibited monolayer and polygonal phenotypes, and acquired fibroblastic cell morphology like primate CECs (Fig. 6A). However, consistent with the primate CECs when the CECs were cultivated with the specific inhibitor to the TGF-β receptor (SB431542), the inhibitor was able to block alteration of the cell shape to fibroblastic phenotypes. Similar to the inhibitory effect of SB431542 on fibroblastic phenotypes, both neutralizing antibody to TGF-β (Fig. 6B) and Smad3 inhibitor (Fig. 6C) also blocked cells from acquiring fibroblastic phenotypes. We then tested whether SB431542 was able to maintain endothelial function. The findings shown in Fig. 7A and Fig. 7B demonstrated that blocking the TGF-β receptor signaling enabled the subcellular localization of Na^+/K^+-ATPase and ZO-1 at the plasma membrane and their protein expression to be maintained. Of

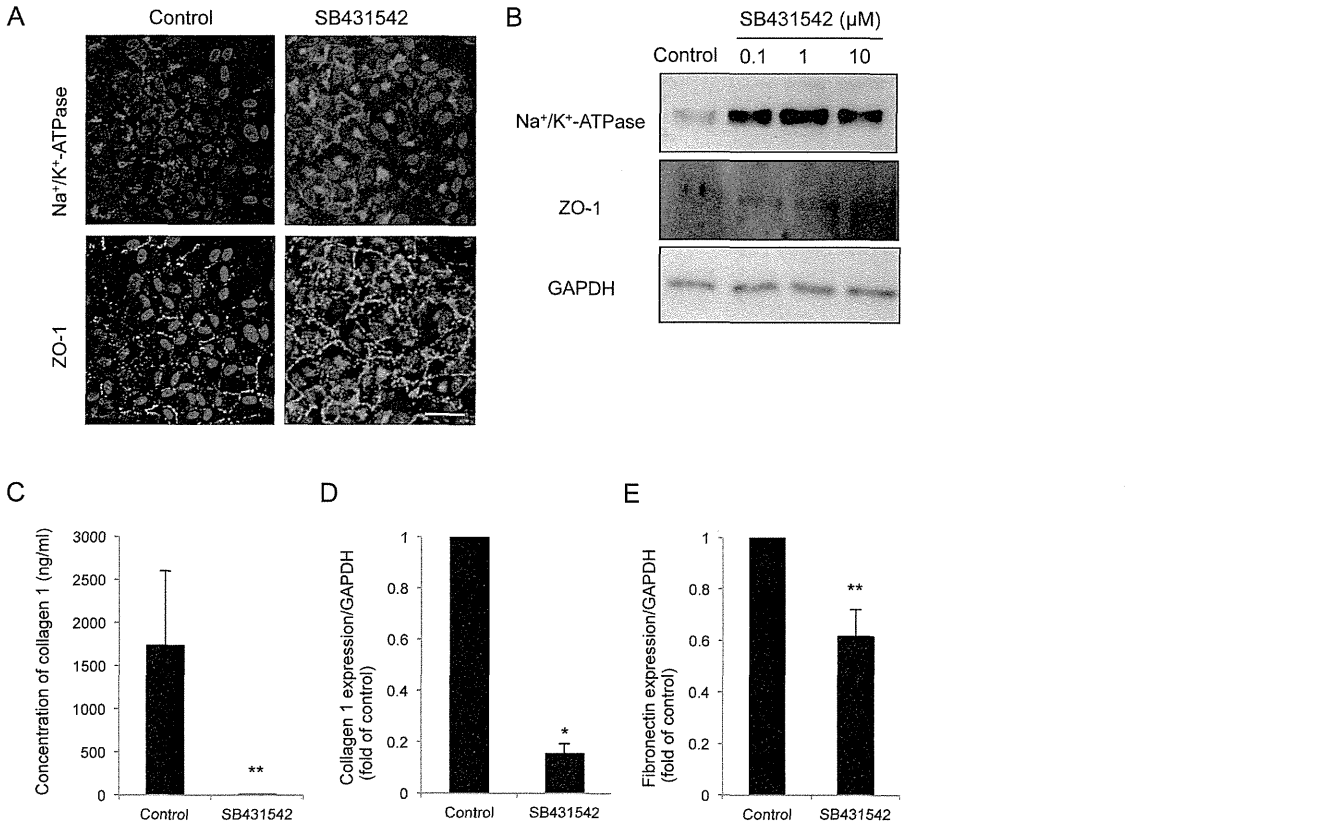

Figure 7. SB431542 maintained the functions and suppressed the fibroblastic change of HCECs. (A+B) Blocking the TGF-receptor signaling by SB431542 (A: 1 μM, B: 0.1, 1, and 10 μM) enabled the subcellular localization of Na^+/K^+-ATPase and ZO-1 at the plasma membrane and their protein expression to be maintained. Scale bar: 100 μm. (C) ELISA assay revealed that SB431542 significantly downregulated the secretion of type I collagen to the culture supernatant. **P<0.05. (D+E) Quantitative PCR showed that SB431542 significantly reduced the expression of type I collagen and fibronectin at the mRNA level. *$p<0.01$, ** $p<0.05$. Samples were prepared in duplicate. Immunoblotting, ELISA, and quantitative PCR were performed in duplicate.
doi:10.1371/journal.pone.0058000.g007

great importance, ELISA assay revealed that SB431542 markedly downregulated the secretion of type I collagen to the culture supernatant (Fig. 7C). Coincidentally, SB431542 markedly reduced the expression of type I collagen and fibronectin at the mRNA level (Fig. 7D, E).

Use of BMP-7 to suppress fibroblastic changes and maintain endothelial functions

Bone morphogenetic protein-7 (BMP-7) promotes MET and specifically inhibits the TGF-β-mediated epithelial-to-mesenchymal transition. Thus, that molecule has been used to antagonize the EMT process [31–34]. We therefore tested whether BMP-7 was able to antagonize the prerequisite changes of HCECs. The fibroblastic HCECs were treated with BMP-7 in a concentration ranging from 10 to 1000 ng/ml. Of important note, the elongated cell shapes of the fibroblastic phenotypes were reversed to the polygonal cell morphology in response to the presence of BMP-7 in a concentration-dependent manner (Fig. 8A). BMP-7 enabled the hexagonal cell morphology and actin cytoskeleton distribution at the cortex to be maintained (Fig. 8B), similar to that observed in normal CECs [35], and it also maintained the subcellular localization of Na^+/K^+-ATPase (Fig. 8C) and ZO-1 (Fig. 8D) at the plasma membrane. Thus, BMP-7 at the concentration of 1000 ng/ml was able to maintain CECs in polygonal and contact-inhibited phenotypes with a positive expression of function-related markers (Fig. 8E, F).

Discussion

Corneal endothelial dysfunction accompanied by visual disturbance is a major indication for corneal transplantation surgery [36,37]. Though corneal transplantation is widely performed for corneal endothelial dysfunction, researchers are currently seeking alternative methods to restore healthy corneal endothelium. The fact that corneal endothelium is cultured and stocked as 'master cells' from young donors allows for the transplantation of CECs with high functional ability and for an extended period of time. In addition, an HLA-matching transplantation to reduce the risk of rejection [38,39] and overcoming the shortage of donor corneas might be possible. Tissue bioengineering is a new approach to develop treatments for patients who have lost visual acuity [40]. To date, there are two methods that utilize bioengineering approaches: 1) use of cultured donor HCECs adhered on bioengineered constructs [4,5,7,9], and 2) transplantation of cultivated HCECs into the anterior chamber [11,41–43]. Regardless of which of the two methods is applied to clinical settings, establishment of an efficient cultivation technique for HCECs is essential and inevitable [44]. Many researchers have noticed that establishing a consistent long-term culture of HCECs is challenging [40]. Although the successful cultivation of HCECs has been reported by several groups, the procedures involved in the isolation and subsequent cultivation protocols varied greatly between laboratories [44]. One of the most difficult problems is

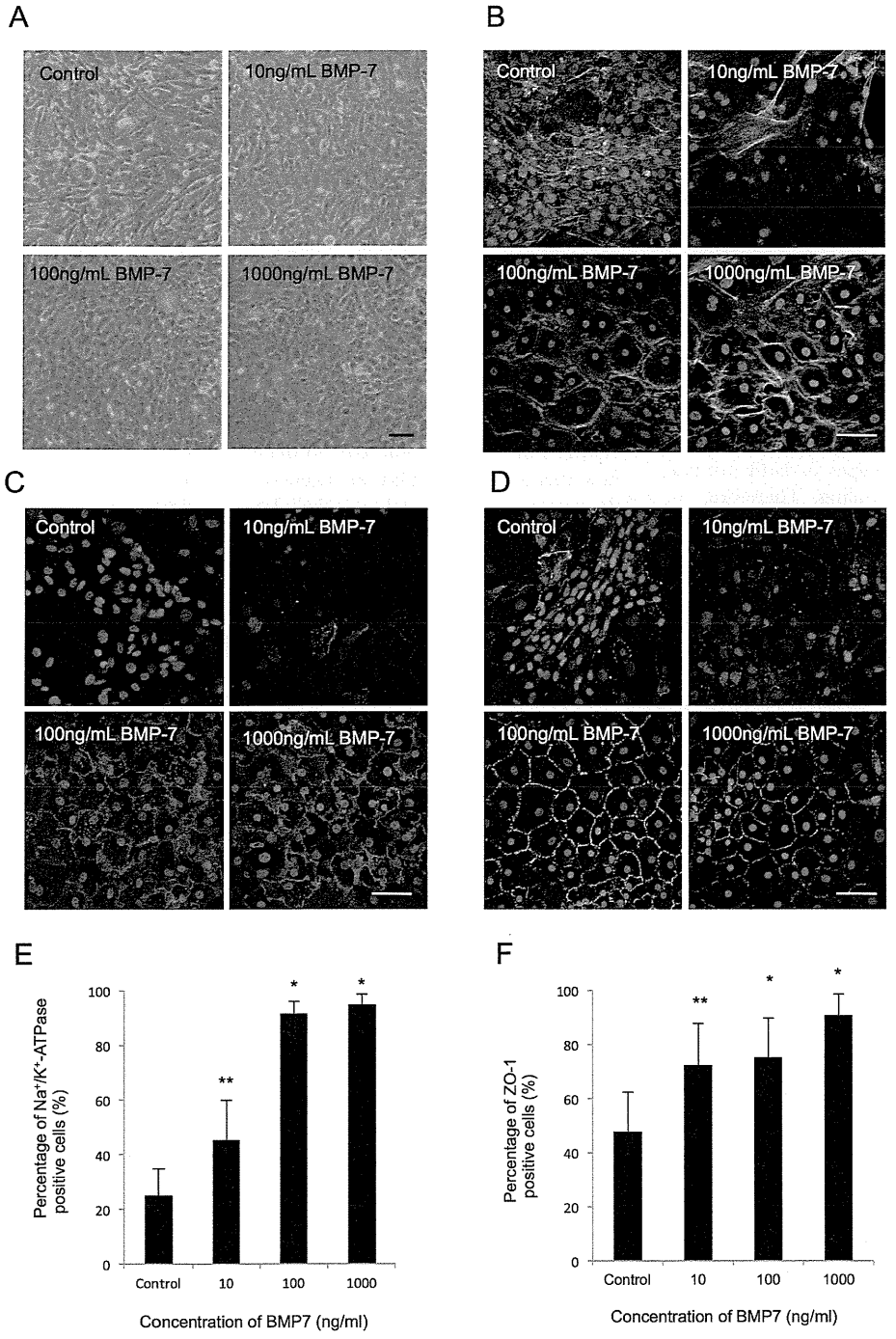

Figure 8. BMP7 suppressed fibroblastic change and maintained the functions of HCECs. (A) The elongated cell shapes of the fibroblastic phenotypes were reversed to a polygonal cell morphology in response to the presence of BMP-7 in a concentration-dependent manner. Scale bar: 50 μm. (B) BMP-7 enabled normal hexagonal cell morphology and actin cytoskeleton distribution at the cortex to be maintained. Scale bar: 100 μm. (C+D) BMP-7 maintained the subcellular localization of Na^+/K^+-ATPase and ZO-1at the plasma membrane. Scale bar: 100 μm. (E+F) The percentages of both Na^+/K^+-ATPase and ZO-1 positive cells treated with BMP-7 were significantly higher than in the control. * $p<0.01$, ** $p<0.05$. The experiment was performed in duplicate.
doi:10.1371/journal.pone.0058000.g008

that HCECs are vulnerable to undergoing massive fibroblastic change over each passage [40]. Therefore, it is essential to find means to circumvent the spontaneous transformation of the CECs in order to maintain the physiological phenotypes for the subsequent use for transplantation.

Transformation of endothelial cells to fibroblastic cells is designated as endothelial- mesenchymal transformation. Such transformation is triggered by TGF-β via the Smad2/3 pathway [16]. Endothelial-mesenchymal transformation causes the loss of the characteristic endothelial phenotypes, such as loss of the contact-inhibited monolayer and loss of the apical junctional